

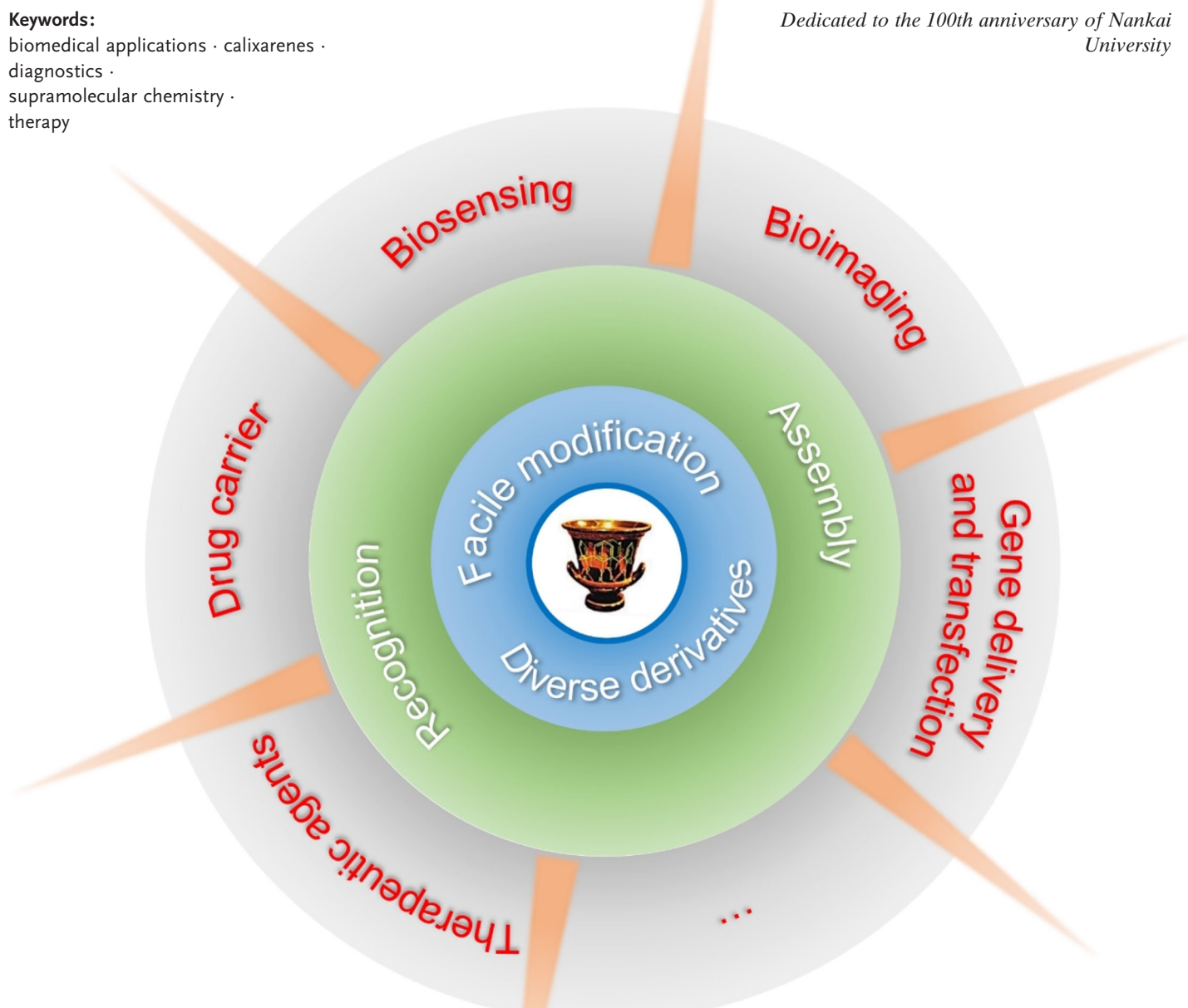
# Biomedical Applications of Calixarenes: State of the Art and Perspectives

Yu-Chen Pan, Xin-Yue Hu, and Dong-Sheng Guo\*

**Keywords:**

biomedical applications · calixarenes ·  
diagnostics ·  
supramolecular chemistry ·  
therapy

Dedicated to the 100th anniversary of Nankai University



**C**alixarenes (CAs), representing the third generation of supramolecular hosts and one of the most widely studied macrocyclic scaffolds, offer (almost) unlimited structure and application possibilities due to their ease of modification, which allows one to establish a large molecular library as a material basis for diverse biomedical applications. Moreover, CAs and their derivatives engage in various noncovalent interactions for the facile recognition of guests including bioactive molecules and are also important building blocks for the fabrication of supramolecular architectures. In view of their molecular recognition and self-assembly properties, CAs are extensively applied in biosensing, bioimaging, and drug/gene delivery. Additionally, some CA derivatives exhibit biological activities and can therefore be used as new therapeutic agents. Herein, we summarize the diverse biomedical applications of CAs including *in vitro* diagnosis (biosensing), *in vivo* diagnosis (bioimaging), and therapy.

## 1. Introduction

Over the past decades, supramolecular chemistry has become strongly linked to the life sciences.<sup>[1]</sup> Molecular recognition and self-assembly processes, such as those involved in phosphate and carbohydrate recognition,<sup>[2]</sup> nucleic acid assembly,<sup>[3]</sup> and protein folding,<sup>[4]</sup> play important roles in biological systems, which has inspired the development of numerous artificial supramolecular systems with rich architectures and functions,<sup>[5]</sup> as exemplified by enzyme mimics,<sup>[6]</sup> artificial channels,<sup>[7]</sup> and artificial viruses.<sup>[8]</sup> As a natural feedback to life systems, biomedical applications are a significant functional output of supramolecular chemistry, encompassing supramolecular biomedical materials,<sup>[9]</sup> supramolecular medicine,<sup>[10]</sup> supramolecular chemotherapy,<sup>[11]</sup> supramolecular theranostics,<sup>[12]</sup> and self-assembling prodrugs,<sup>[13]</sup> to name just a few. The past decades have witnessed progress in supramolecular chemistry that paves the way to precision (or personalized) medicine. Compared to covalent approaches, noncovalent ones display several advantages, e.g., they avoid tedious syntheses and complicated purification procedures, and are thus environmentally friendly as well as time- and cost-effective.<sup>[14]</sup> Moreover, the dynamic nature of noncovalent interactions allows for the convenient dissociation and reconstruction of supramolecular materials, enabling their recycling and self-healing. Additionally, the certain adaptability of noncovalent interactions in response to external stimuli can be used for the design and fabrication of stimuli-responsive materials. Finally, supramolecular chemistry uses the “bottom-up” principle and thus provides an alternative way of controlling material size and morphology.

Macrocycles like crown ethers, cyclodextrins (CDs), calixarenes (CAs), cucurbiturils, and pillararenes are important objects of study in supramolecular chemistry. Among them, CDs are the most widely investigated supramolecular hosts, comprising oligosaccharides linked by  $\alpha$ -1,4 glycosidic bonds and featuring good solubility in water, molecular recognition and self-assembly abilities, and biocompatibility. These prop-

## From the Contents

<b>1. Introduction</b>	2769
<b>2. Overview of Calixarenes</b>	2770
<b>3. Toxicity</b>	2771
<b>4. Biosensing</b>	2772
<b>5. Bioimaging</b>	2778
<b>6. Drug Carriers</b>	2779
<b>7. Gene Delivery and Transfection</b>	2782
<b>8. Therapeutic Agents</b>	2783
<b>9. Summary and Outlook</b>	2788

erties make CDs well suited for biomedical applications, such as drug delivery, gene therapy, bioimaging, and pharmaceuticals from the viewpoints of both scientific research and industry.<sup>[15]</sup>  $\alpha$ -,  $\beta$ -, and  $\gamma$ -CDs are listed in the Japanese Pharmacopoeia, while  $\alpha$ - and  $\beta$ -CDs are also listed in the European Pharmacopoeia. Moreover,  $\beta$ -CD is listed in the U.S. Pharmacopoeia and is generally recognized as safe by the Food and Drug Administration.<sup>[16]</sup> In the 1950s, CDs were reported to enhance the solubility and stability of drugs via host-guest complexation.<sup>[17]</sup> In 1976, the first CD-containing pharmaceutical product was marketed in Japan (Prostarmon E<sup>TM</sup> sublingual tablets). After 12 years, CD-containing products appeared on the European market, making their way into the U.S. in 1997. To date, at least 54 CD-containing pharmaceutical products are in clinical trials or have even been clinically approved (<https://www.clinicaltrials.gov/>). The success of CDs has inspired the development of several other macrocycles for application in biomedical fields, namely calixarenes, cucurbiturils, pillararenes, and cavitands.<sup>[12b,18]</sup> Although the clinical use of these macrocycles is currently (end of 2019) not extensively characterized, early studies have suggested the broad prospects of these macrocycles for various biomedical applications.<sup>[9,14]</sup>

CAs, representing the third generation of supramolecular hosts, are macrocycles comprising phenolic units linked by methylene groups at positions 2 and 6.<sup>[19]</sup> These compounds have been described as macrocycles with (almost) unlimited

[\*] Y.-C. Pan, Dr. X.-Y. Hu, Prof. Dr. D.-S. Guo

College of Chemistry, Key Laboratory of Functional Polymer Materials (Ministry of Education), State Key Laboratory of Elemento-Organic Chemistry, Nankai University  
Tianjin 300071 (China)  
E-mail: dshguo@nankai.edu.cn

 The ORCID identification number(s) for the author(s) of this article can be found under:  
<https://doi.org/10.1002/anie.201916380>.

structure and application possibilities, because they possess tunable scaffolds and controllable conformations, and can be easily modified.<sup>[20]</sup> The abundance of CA derivatives with diverse recognition and assembly properties results in diverse biomedical applications.<sup>[21]</sup> Despite the availability of several pivotal reviews on the biomedical applications of CAs,<sup>[21,22]</sup> most of them mainly focus on only one aspect, and only few of them are comprehensive, which is especially important given the fast progress in this field. In view of the above, we herein systematically summarize the typical biomedical applications of CAs, such as in vitro diagnosis (biosensing), in vivo diagnosis (bioimaging), and therapy (drug delivery, gene transfection, therapeutic agents), discussing the potential challenges and perspectives of this field. Moreover, we provide a short overview of CAs for readers less familiar with these hosts and illustrate CA toxicity in consideration of their biomedical applications. Although every effort has been made to demonstrate the diverse biomedical applications of CAs with the help of representative works, this review cannot be viewed as fully inclusive, as missing some related works is inevitable.

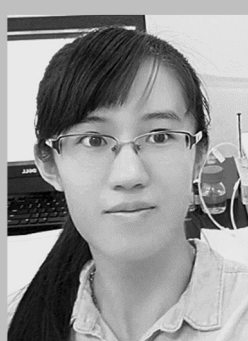
## 2. Overview of Calixarenes

In 1872, Adolph von Bayer reported the first results concerning products obtained from the reaction of phenol with formaldehyde.<sup>[23]</sup> However, he failed to isolate or characterize these products after numerous attempts. In 1944, Zinke and Ziegler blocked the *para*-position of phenol by using *para*-*tert*-butylphenol and proposed a cyclic tetramer structure for the product of its reaction with formaldehyde.<sup>[24]</sup> After the 1970s, Gutsche demonstrated the presence of cyclic homologues, in particular the tetramer,

hexamer, and octamer, by NMR spectroscopy, showing how the most common CA macrocycles can be obtained in good yield and with high selectivity under appropriate conditions (base, solvent, temperature, etc.).<sup>[25]</sup> Besides, Gutsche first proposed the name “calixarenes” by structural analogy with the form of the ancient Greek calix-krater vases. This name is now generally used, because the systematic IUPAC terminology is too complicated. The simplified nomenclature of CAs uses  $[n]$  to denote the number of phenolic units in the macrocycle (calix[ $n$ ]arene, C $n$ A); for example, C4A contains four units.

The facile derivatization of CAs is one of the key features that makes them unique among other macrocycles. The hydroxyl groups at the lower rim provide excellent handles for the incorporation of other moieties via reactions with electrophiles, as exemplified by O-acylation and O-alkylation.<sup>[20]</sup> For the upper rim, almost all common substitutions possible for phenols/phenol ethers have been carried out for CAs or their alkyl ether derivatives, e.g., halogenation, nitration, sulfonation, sulfochlorination, and coupling with diazonium salts.<sup>[20]</sup> The methylene bridge can be brominated by *N*-bromosuccinimide to prepare a wide array of methylene-modified derivatives.<sup>[26]</sup> Methylene-bridge-substituted CAs can also be obtained by stepwise synthesis.<sup>[27]</sup> Furthermore, one can also replace the methylene bridge carbon with other atoms, such as sulfur and oxygen.<sup>[28]</sup> Control over the number and position of introduced substituents allows one to synthesize a plethora of CA derivatives.<sup>[20,21]</sup> Moreover, considering the tunable scaffold and controllable conformation, one can establish a large molecular library of CA derivatives (Scheme 1) as a material basis for biomedical applications.

Recognition and assembly are two important aspects of supramolecular chemistry. CA cavities can provide multiple



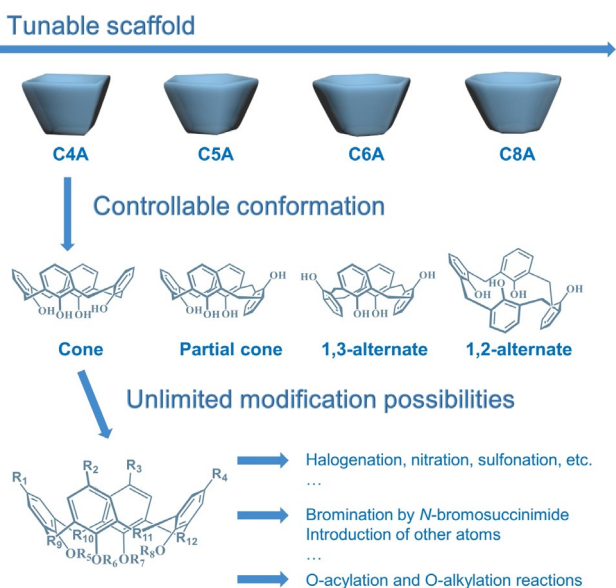
Yu-Chen Pan obtained her BSc (2016) degree from Nankai University. Since 2016 she has been working towards a PhD at College of Chemistry, Nankai University. She is interested in thermodynamics in recognition, membrane transport, and inhibition of amyloid fibrillation based on calixarenes.



Dong-Sheng Guo obtained his PhD degree from Nankai University under the guidance of Prof. Yu Liu in 2006. Then he joined Prof. Liu's group as a faculty member at College of Chemistry, Nankai University. He was promoted as an Associate Professor in 2008, and a full Professor in 2013. In 2014, he began independent research. The current research interest in his group is supramolecular biomedical materials.



Xin-Yue Hu obtained her BSc (2012) and MSc (2015) degrees in organic chemistry from Nankai University and PhD (2019) degree in organic chemistry from Heidelberg University under the guidance of Prof. Michael Mastalerz. Since 2019 she has been carrying out postdoctoral research in the group of Prof. Dong-Sheng Guo at Nankai University. Her current research focuses on bioimaging and fluorescence sensing based on macrocyclic receptors.



**Scheme 1.** Representation of the large molecular library derivable from CAs.

noncovalent (hydrophobic,  $\pi\cdots\pi$  stacking, cation $\cdots\pi$ , and  $\text{CH}\cdots\pi$ ) interactions,<sup>[29]</sup> while CA conformations can be kept mobile to exploit induced-fit binding or be finely locked in pre-organized structures for more specific binding.<sup>[22a,30]</sup> CAs can recognize guests of various sizes. For example, C4A is suitable for small guests, while C8A is suitable for larger ones. Furthermore, CA recognition behavior is largely dependent on decorating groups. For example, the introduction of negatively charged sulfonate or carboxyl groups provides electrostatic as well as hydrogen-bonding interaction sites, resulting in strong affinity for cationic guests.<sup>[31]</sup> In contrast, CAs modified with positively charged guanidinium units tightly bind various organic and inorganic anions.<sup>[32]</sup> Deep cavitands derived from CAs are capable of encapsulating large hydrophobic guests.<sup>[22e]</sup> In addition, the recognition properties of CAs are due not only to the presence of cavities, because the modification of CA scaffolds with individual ligands to afford podand-like structures also plays a significant role in molecular recognition.<sup>[33]</sup> Thus, the variability of scaffolds, conformations, and substitution patterns allows CAs to bind a wide range of guests, such as inorganic anions,<sup>[34]</sup> inorganic cations,<sup>[35]</sup> organic anions,<sup>[36]</sup> organic cations,<sup>[37]</sup> neutral organic molecules,<sup>[38]</sup> and biological macromolecules.<sup>[39]</sup>

In addition to exhibiting recognition properties, CAs are also important building blocks for the fabrication of supramolecular architectures, such as micelles, vesicles, nanofibers, tubes, capsules, cages, rotaxanes, catenanes, supramolecular polymers, solid lipid nanoparticles, and liquid crystals.<sup>[40]</sup> Among the various assemblies, CA-based amphiphiles, which can be obtained by simple modification of hydrophilic/hydrophobic groups on upper/lower rims, are most frequently engaged in biomedical applications. Macrocylic amphiphiles are a type of pre-organized cyclic oligomers of amphiphiles, comprising multiple hydrophilic residues at one

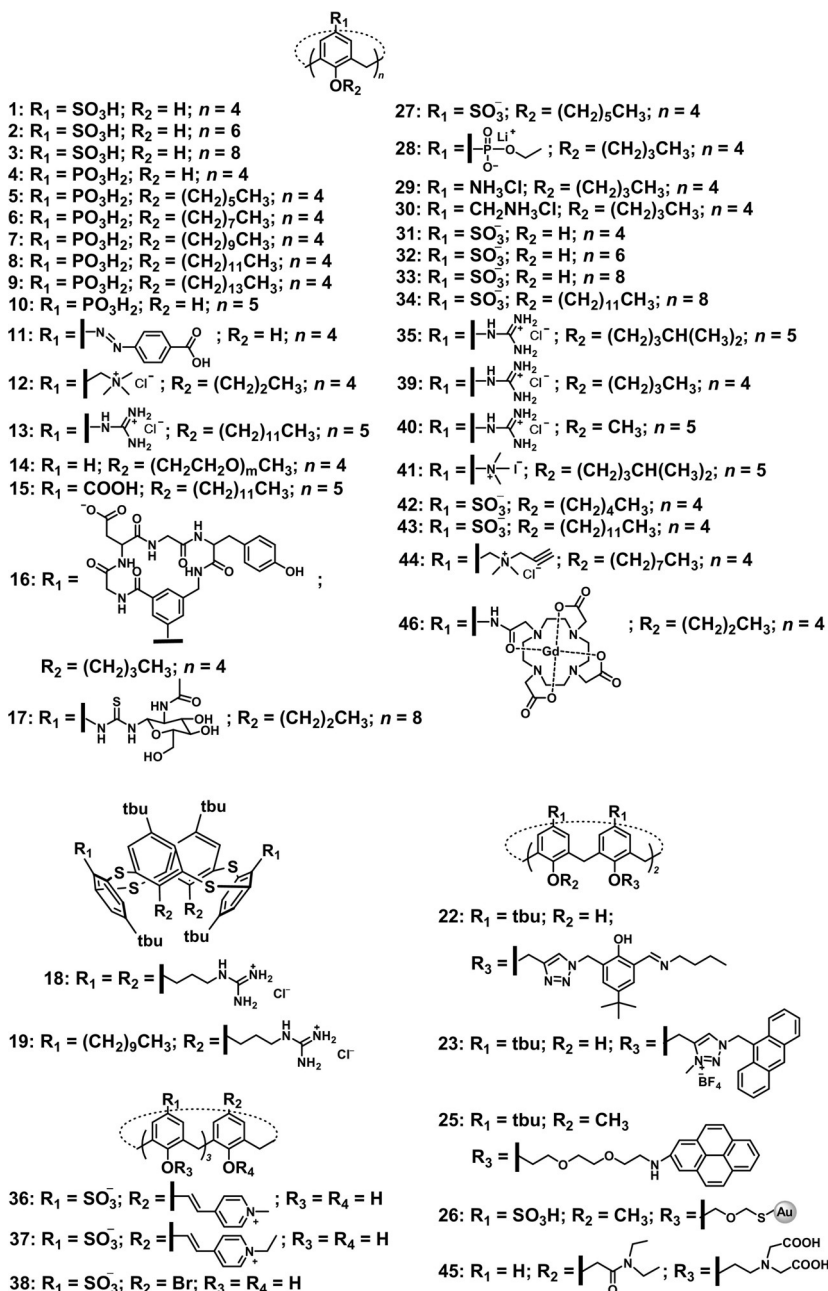
rim and multiple lipophilic residues at the other rim, thus containing both bola- and gemini-type amphiphiles in a single molecule from the viewpoint of structural characteristics and exhibiting superior host-guest recognition properties.<sup>[40a,41]</sup> Unsurprisingly, macrocyclic amphiphiles, integrating recognition and assembly, have been denoted as “surfactants with host-guest recognition sites” and represent a new matrix for biomedicine.<sup>[42]</sup> Compared to other macrocycles, CAs are easy to modify, providing plentiful building blocks. For example, more than 400 CA amphiphiles have been reported.<sup>[40b]</sup> Additionally, CAs can form supra-amphiphiles via CA-induced aggregation.<sup>[22d,40a,43]</sup> Hydrophilic CAs can promote the self-aggregation of aromatic or amphiphilic molecules by lowering their critical aggregation concentration (CAC), enhancing aggregate stability and compactness, and regulating the degree of order in aggregates.<sup>[44]</sup> The fascinating assembly behavior, along with the aforementioned recognition properties, especially for biological substrates, provides supramolecular approaches to realizing biomedical applications of CAs.

### 3. Toxicity

Since the toxicity of a given compound largely determines its biomedical application potential, we first discuss CA toxicity before moving on to the corresponding biomedical applications, focusing on the balance of dose and curative effect. Currently, the cytotoxicity, hemolytic activity, inflammation, metabolism, and other properties of some CA derivatives have been well studied.<sup>[31a,45]</sup> CA toxicity depends on the appended groups and can therefore be regulated accordingly.

Most CAs are remarkably nontoxic.<sup>[22a]</sup> *p*-Sulfonatocalix-[*n*]arenes (*n* = 4, 6, 8, **1–3** in Scheme 2) are a prominent family of water-soluble CA derivatives with numerous biomedical applications and extensively studied toxicities. In 2004, Coleman et al. reported that **1** exhibits no hemolytic effects at concentrations of up to 200 mM.<sup>[46]</sup> For **2** and **3**, although hemolytic effects were observed at the above concentration, they were significantly reduced at lower concentrations. In 2006, Coleman et al. claimed that **1–3** show no activation of neutrophils, i.e., do not illicit an immune response, even at relatively high concentrations.<sup>[47]</sup> In 2008, these authors studied the *in vivo* toxicity of **1** and confirmed that this species exhibited no toxicity at doses of up to 100 mg kg<sup>−1</sup>.<sup>[48]</sup> In 2009, Wheate et al. examined the cytotoxicity of **1** using *in vitro* growth inhibition assays in A2780 and A2780cis (corresponding cisplatin-resistant daughter line) human ovarian cancer cell lines, revealing that **1** displays no cytotoxicity at concentrations of up to 1.5 mM.<sup>[49]</sup> Dunlop et al. reported that a series of *p*-phosphonic acid C*n*As (*n* = 4 and 5) bearing hydroxyl groups or variable-length alkyl chains at lower rims (**4–10**) had almost no toxicity.<sup>[50]</sup> The authors examined the effect of these compounds on the viability of rat PC12 cells, showing that no effect was observed at concentrations up to 1 mg mL<sup>−1</sup>. Our group recently reported a carboxyl-modified azocalix[4]arene (**11**) with negligible cytotoxicity against A549 cells even at 50  $\mu\text{M}$ .<sup>[51]</sup> Loftsson et al. examined the

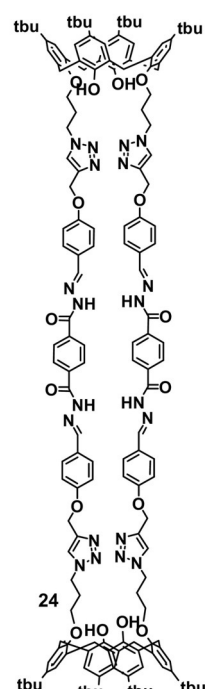
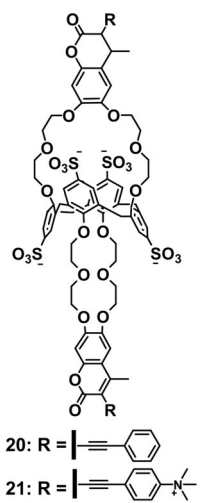
152 | [10.1002/jane.20196380](https://doi.org/10.1002/jane.20196380), Downloaded from <https://onlinelibrary.wiley.com/doi/10.1002/jane.20196380> by University Of Science, Wiley Online Library on [14/07/2024]. See the Terms and Conditions (<https://onlinelibrary.wiley.com/terms-and-conditions>) on Wiley Online Library for rules of use; OA articles are governed by the applicable Creative Commons License.



**Scheme 2.** Molecular structures of CAs (1–46) mentioned in this Review.

cytotoxicity and hemolytic effect of an amphiphilic tetraalkylammonium-modified C4A (**12**), revealing the absence of cytotoxicity up to 200  $\mu\text{M}$  in tests on mouse macrophage RAW 264.7 cells.<sup>[52]</sup> In terms of hemolytic activity toward rabbit red blood cells, **12** was not active at concentrations of up to 100  $\mu\text{M}$ . In addition, assemblies based on amphiphilic CAs (**13**, **14**, and **15**) were shown to exhibit no or negligible cytotoxicity and in vivo toxicity by us and other groups.<sup>[53]</sup>

The toxicity of some CA derivatives can be useful in certain cases. Sebti and Hamilton reported significantly cytotoxic C4A derivatives that could inhibit tumor growth and angiogenesis, with the lowest IC<sub>50</sub> observed for **16**.<sup>[54]</sup> Viola et al. reported that C8A carrying an *N*-acetyl-D-glucosamine group (**17**) inhibits glioma cell migration and proliferation, and is thus a potential novel anticancer drug.<sup>[55]</sup> Most



certainly, some CA derivatives also show toxicity to normal cells and thus are suitable for only limited applications. Galukhin et al. reported the cytotoxicity of guanidinium-modified thiocalix[4]arenes in a 1,3-alternate conformation (**18** and **19**).<sup>[56]</sup> Three cell lines (monkey kidney, saiga kidney, and L-mouse fibroblast) were employed, and IC<sub>50</sub> values of  $\approx 1 \mu\text{M}$  were obtained.

CA toxicity is a double-edged sword. Both toxic and nontoxic derivatives are useful, depending on the intended application. In vitro sensing applications generally do not place restrictions on (non)cytotoxicity. Nontoxic CAs can be used for *in vivo* imaging and drug delivery, while toxic CAs can be used as therapeutic agents for some diseases. Of course, one expects that toxic CAs are targeted and specific to lesion tissues. For other CAs, toxicity is demonstrated below in the discussion of relevant biomedical applications.

## **4. Biosensing**

The sensing of biomolecules is critical for the early screening of diseases and accurate diagnosis, facilitating effective treatment and even improving patient survival rates. Biomolecules are substances found in blood, urine, stool, or tissues, and are generally ions, amino acids, proteins, or neurotransmitters. As a kind of artificial receptors, CAs possess discrete cavities selective for the complementary binding of certain guests. At the same time, unlimited modification possibilities also allow for recognition based on podand-like ligands. Hence, CA derivatives have drawn

considerable attention and significantly contributed to the field of host–guest recognition.<sup>[57]</sup> Kim and Gibb have reviewed CA-based fluorescent receptors, focusing on those for metal ions and anions.<sup>[22k]</sup> However, the use of CAs for sensing other biomolecules has not been comprehensively summarized. Herein, because of space limitations, we review the applications of CAs in biosensing, focusing on cases where CAs directly interact with analytes. These applications can be classified into direct and competitive sensing, depending on whether competitive complexation occurs during the sensing process.<sup>[58]</sup> Moreover, we discuss the applications of CAs in supramolecular tandem assay (STA), a recently developed time-resolved version of competitive sensing.<sup>[59]</sup> One should also note the abundance of research on drug sensing to guide dose adjustment and solve problems such as microbial resistance.<sup>[60]</sup> This research will not be discussed in detail herein, because it does not contribute to the field of diagnosis.

#### 4.1. Direct Sensing

Direct sensing features signaling and recognition units as two indispensable components. Analyte binding induces a signal change, and vice versa, signal measurements can be employed to explore guest binding (Scheme 3).<sup>[58]</sup> Most direct sensing systems based on CAs correspond to podand-like ligands.<sup>[61]</sup> Usually, two or more functional groups are appended to the CA scaffold to enable interaction with analytes and the induction of a signal change (Scheme 3a).

Leray et al. synthesized two CA derivatives (**20** and **21**) for the sensing of K<sup>+</sup>.<sup>[62]</sup> When these compounds complex K<sup>+</sup> via their crown ether rings, the two sulfonate groups move toward the cation because of electrostatic attraction, which increases the charge density around the crown ring oxygens and the charge transfer efficiency of coumarin, resulting in a red-shifted absorption spectrum and enhanced fluorescence (Figure 1a). Notably, **20** had no effect on neuronal activity

and was applied to monitor extracellular K<sup>+</sup> levels. Rao et al. reported C4A derivatives (**22** and **23**) for the sensing of Zn<sup>2+</sup><sup>[63]</sup> and biological phosphates,<sup>[64]</sup> respectively, showing that complexation with analytes enhanced the fluorescence of **22** and **23** (Figure 1b,c). Shah et al. reported that the fluorescence of **24** was quenched in the presence of Cu<sup>2+</sup> (Figure 1d) and used this behavior to detect Cu<sup>2+</sup> in drinking water and living cells.<sup>[65]</sup> Menon et al. reported a tryptophan (Trp) and histidine (His) sensing system based on a substituted C4A fluoroionophore (**25**).<sup>[66]</sup> The addition of Trp to a solution of **25** resulted in fluorescence enhancement, while His induced fluorescence quenching (Figure 1e). Benefiting from high association constants, this sensing system exhibited high selectivity and sensitivity, and was successfully applied for the selective detection of Trp and His in blood serum.

In addition to acting as scaffolds for podand-like ligands, CAs also provide cavities as recognition units (Scheme 3b). Thiol-functionalized CAs can be easily attached to the surface of Au nanoparticles (AuNPs), which strongly absorb in the visible region and exhibit color-tunable behavior. CA-functionalized AuNPs have been used to sense various analytes.<sup>[68]</sup> For example, Menon et al. employed them for the colorimet-

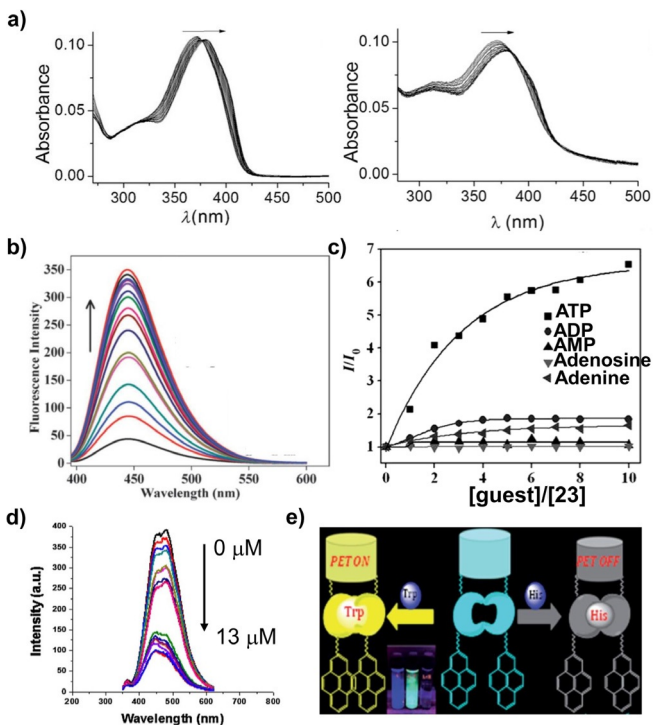
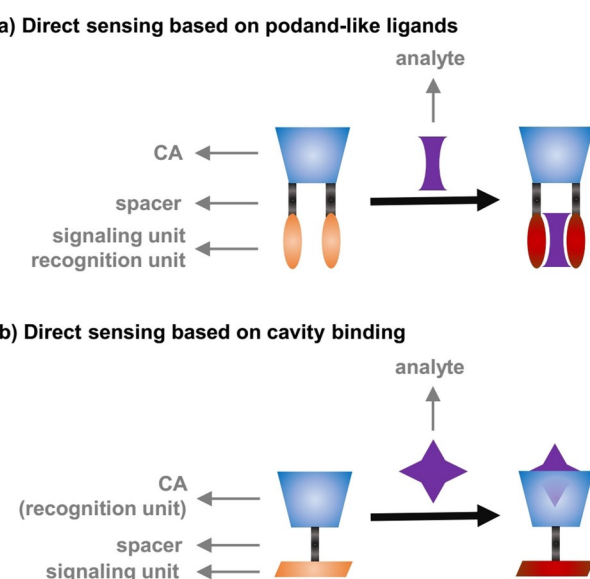


**Figure 1.** a) Absorption spectra of **20** (left) and **21** (right) in water upon addition of K<sup>+</sup>. Reprinted with permission from ref. [62]. Copyright 2016 Wiley-VCH Verlag GmbH & Co. KGaA, Weinheim. b) Fluorescence spectra of **22** in water:methanol (1:4, v/v) HEPES buffer at pH 7.4 upon addition of Zn<sup>2+</sup>. Reprinted with permission from ref. [63]. Copyright 2010 Royal Society of Chemistry. c) Relative fluorescence intensity ( $I/I_0$ ) as a function of the [guest]/[23] molar ratio. Reprinted with permission from ref. [64]. Copyright 2014 Wiley-VCH Verlag GmbH & Co. KGaA, Weinheim. d) Fluorescence spectra of a solution of **24** in tap water upon addition of Cu<sup>2+</sup>. Reprinted with permission from ref. [65]. Copyright 2016 Elsevier. e) Schematic design of **25** as a probe for Trp and His. Reprinted with permission from ref. [66]. Copyright 2014 Royal Society of Chemistry.



**Scheme 3.** Schematic representation of direct sensing based on CAs.

ric sensing of creatinine, which is an indicator of kidney problems.<sup>[68c]</sup> Compound **26** was grafted onto AuNPs, and its complexation with creatinine resulted in nanoparticle aggregation and, hence, in color changes (Figure 2a). The practical applicability of this system was confirmed by the reliable and accurate sensing of creatinine in human urine.

In addition to the covalent tethering of signaling units to CA, their noncovalent grafting can also be used to achieve responsiveness to the desired analytes. Jin et al. modified CdSe/ZnS quantum dots (QDs) with an amphiphilic CA derivative (**27**) to sense acetylcholine (ACh) based on the fluorescence quenching observed upon complexation of **27**

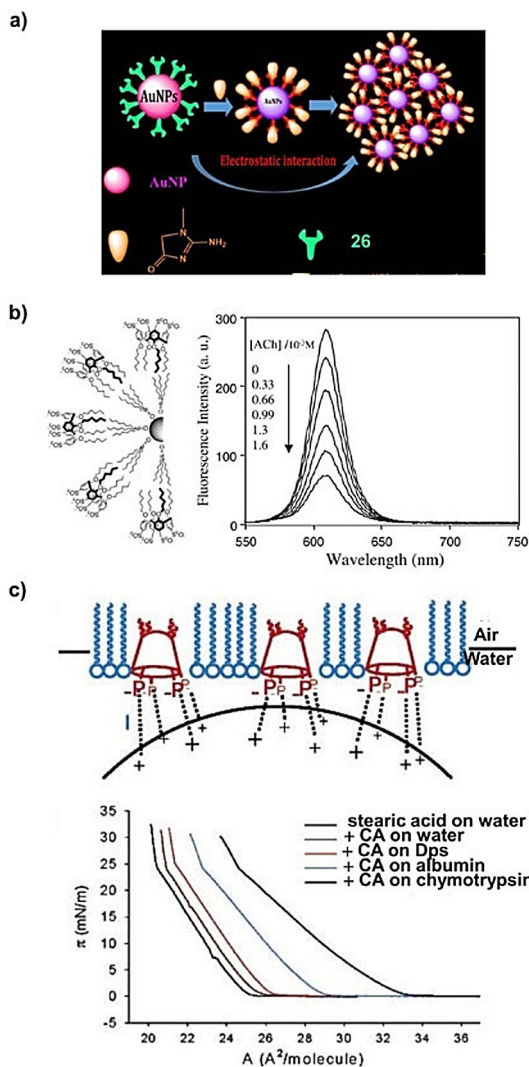


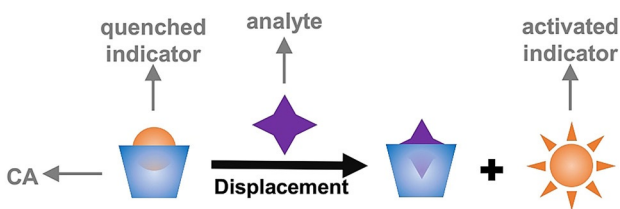
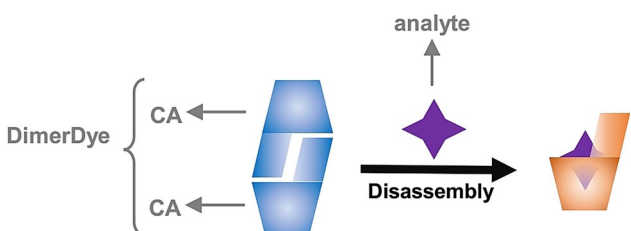
**Figure 2.** a) Schematics of creatinine sensing by **26**-modified AuNPs. Reprinted with permission from ref. [68c]. Copyright 2016 Elsevier. b) Left: Schematic illustration of CdSe/ZnS QDs coated with **27**. Right: Quenching of the fluorescence emission of **27**-coated CdSe/ZnS QDs upon ACh addition. Reprinted with permission from ref. [69]. Copyright 2005 Royal Society of Chemistry. c) Top: Proposed mode of binding between embedded **28** and basic proteins in the aqueous subphase. Bottom: Langmuir isotherms obtained for  $\approx 10^{-8}$  M protein solutions and **25** incorporated into a stearic acid monolayer at the air–water interface. Reprinted with permission from ref. [70b]. Copyright 2005 American Chemical Society.

with ACh (Figure 2b).<sup>[69]</sup> The quenching process featured contributions from both static and dynamic mechanisms and the dynamic mechanism was the main contributor. Schrader et al. reported systems for sensing various basic proteins.<sup>[70]</sup> Amphiphilic **C4A** (**28**) showed high affinities to arginine (Arg)- and/or lysine (Lys)-rich proteins and could be incorporated into a stearic acid monolayer on water, benefiting from amphipathy. The addition of basic proteins to the mixed monolayer produced moderate but distinct additional expansions of pressure/area diagrams because of complexation with **28** (Figure 2c). Subsequently, cationic CAs containing amino groups (**29** and **30**) were introduced to realize the sensing of acidic proteins by the same strategy.<sup>[71]</sup> On the basis of the above research, Schrader et al. co-assembled a phospholipid with polydiacetylene, which changed color from blue to red in response to stimuli such as heat, ionic strength, and mechanical pressure.<sup>[72]</sup> The addition of proteins in the presence of CAs caused an obvious color change and thus allowed for protein detection by the naked eye.

#### 4.2. Indicator Displacement Assay (IDA) and Differential Sensing

Competitive binding, in which a series of guests compete for a receptor, is a well-established approach in supramolecular chemistry. The exploitation of competitive binding for sensing applications, so-called competitive sensing, has a long history and is exemplified by IDA.<sup>[58,73]</sup> In a typical IDA experiment, an indicator is bound to a receptor to create the sensing ensemble, and subsequent analyte introduction causes the displacement of the indicator out of the receptor.<sup>[73]</sup> Since the complexation of CAs with chromophores generally results in changes in optical (fluorescent or colorimetric) signals, the molecular recognition of CAs has been widely used in IDA (Scheme 4a). Recently, Hof proposed the DimerDye disassembly assay (DDA), which also takes advantage of competitive binding (Scheme 4b).<sup>[74]</sup> Competitive sensing is compatible with differential sensing, because the array can be easily constructed by changing receptors/indicators without additional synthetic efforts (Scheme 4c).<sup>[58]</sup>

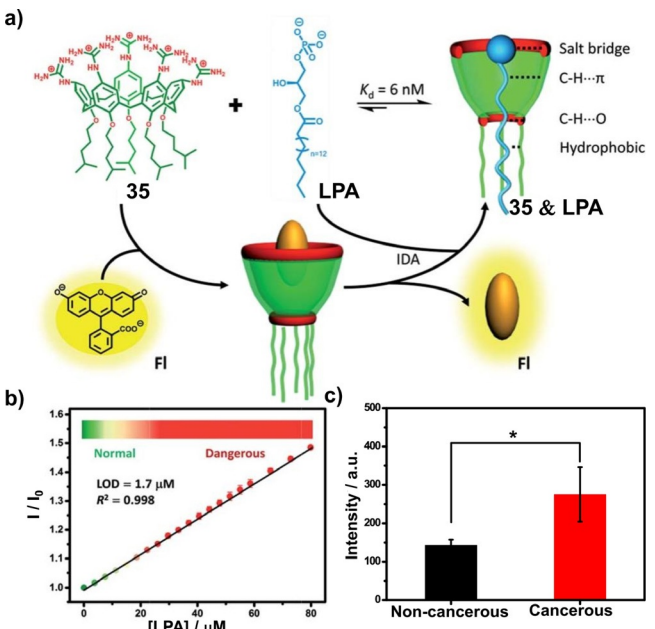
ACh plays a modulatory role in the central nervous system and is involved in the translation of chemical signals into electrical ones. Nau et al. reported a sensing system for ACh, choline, and carnitine based on the IDA strategy, employing *p*-sulfonatocalix[4]arene (**31**) and 2,3-diazabicyclo[2.2.2]oct-2-ene (DBO) as a reporter pair.<sup>[75]</sup> The addition of **31** to DBO solutions resulted in efficient fluorescence quenching, while ACh, choline, and carnitine derivatives caused the regeneration of fluorescence by displacing DBO out of **31**. Yitzchaik et al. studied the role of the CA skeleton in the sensing of ACh using *p*-sulfonatocalix[4,6,8]arenes (**SCnA**, **31**, **32**, **33**) as hosts and *trans*-4-[4-(dimethylamino)styryl]-1-methylpyridinium-*p*-toluenesulfonate (4ASP) as an indicator.<sup>[76]</sup> The association affinities of these reporter pairs equaled  $\approx 10^5 \text{ M}^{-1}$ , and complexation induced a drastic increase (20- to 60-fold) of the fluorescence intensity of 4ASP. Fluorescence titration experiments showed that **32** was the most suitable host, because the cavity of **31** was too small, while that of **33** was too

**a) Indicator displacement assay (IDA)**

**b) DimerDye disassembly assay (DDA)**

**c) Differential sensing**


**Scheme 4.** Schematic presentation of a) IDA, b) DDA, and c) differential sensing.

large and flexible. Jin et al. reported the interfacial sensing of ACh.<sup>[77]</sup> Specifically, **34** was incorporated into dimyristoyl phosphatidylcholine vesicles, and rhodamine 6G (Rh6G) was employed as an indicator. The replacement of ACh with Rh6G resulted in changes of steady-state fluorescence, fluorescence anisotropy, and fluorescence correlation spectroscopy signals. The authors pointed that the selectivity of this vesicle system was not exactly the same as that of the parent compound **34** in homogenous solution, which suggested that membrane potential also played an important role. Jin et al. also employed a near-infrared-fluorescent dye, rhodamine 800, for ACh sensing based on the IDA strategy to increase the suitability of the sensing platform for biological systems.<sup>[78]</sup>

IDA has also been applied to the sensing of other substrates.<sup>[79]</sup> Lysophosphatidic acid (LPA) is a bioactive phospholipid considered to be an ideal biomarker for the early detection of ovarian and other gynecologic cancers.<sup>[80]</sup> Our group has constructed an LPA sensing system based on the IDA strategy, using fluorescein (Fl) as an indicator and guanidinium-modified C5A (**35**), which has a suitable cavity size and can provide salt bridge, C–H···π, C–H···O, and hydrophobic interactions with LPA, as a host (Figure 3a).<sup>[81]</sup> This well-designed system showed excellent selectivity and sensitivity, with an LOD of 1.7 μM, and was employed for the determination of LPA in untreated serum. The linear relationship between fluorescence and LPA concentration



**Figure 3.** a) Schematic illustration of binding between LPA and **35** and the operating principle of the fluorescence “switch-on” sensing of LPA by the **35**-Fl reporter pair. b) The set-up calibration curve used to quantify LPA in serum. c) Comparison of fluorescence signals between blood samples of ovarian cancer-bearing and normal mice. Reprinted with permission from ref. [81]. Copyright 2018 Royal Society of Chemistry.

made it possible to construct a calibration curve to accurately determine the level of LPA even in the low- $\mu\text{M}$  range (Figure 3b). Finally, animal studies proved the possibility of using this sensing system for practical diagnosis (Figure 3c).

IDA displays several advantages such as receptor universality, allowing one to modulate the sensitivity and selectivity of sensing systems. However, one disadvantage of IDA is that various co-solutes, such as NaCl, can reduce performance. Hof et al. reported a refined competitive sensing system based on the self-assembled DimerDye, modifying dyes on CA to form two new merocyanine CAs (**36** and **37**).<sup>[74,82]</sup> Both these CAs self-assembled into non-emissive dimers in aqueous solution, and guest addition resulted in dimer dissociation and turned on fluorescence (Scheme 4b). This strategy, denoted as the DimerDye disassembly assay (DDA), was applied to the sensing of amino acids, and the signal intensity slightly decreased after salt addition.

The differential sensing strategy aims to mimic the mammalian nose and tongue to sense smell and taste, respectively, achieving analyte sensing via the composite response of the entire array of receptors (Scheme 4c). Compared to direct sensing, IDA is more compatible with differential sensing, because one can easily construct an array by changing receptors and/or indicators without additional synthetic efforts. Hof et al. extensively worked on sensing Lys and post-translationally modified Lys,<sup>[83]</sup> reporting a sensor array for differentiation of different degrees of methylation (monomethyl (Lys(Me<sub>1</sub>)), dimethyl (Lys(Me<sub>2</sub>)), and trimethyl (Lys(Me<sub>3</sub>))) and acetylation (Lys(Ac)).<sup>[84]</sup> These authors employed SC4A (**31**), SC6A (**32**), and monobrominated

SC4A (**38**) as receptors, and lucigenin (LCG) and pyridinopyrene as indicators. The addition of different amino acids produced an array of signals, and the obtained data were analyzed by linear discriminant analysis (LDA) (Figure 4). Notably, these amino acids could be well distinguished. The above sensing system was then employed to sense Lys and distinguish its modifications in peptides.

Our group reported the discrimination of glycosaminoglycans (GAGs).<sup>[85]</sup> Four positively charged CA derivatives (**35**, **39–41**) were chosen as hosts, and Eosin Y was chosen as a reporter dye. Six GAGs with slight structural differences, viz. heparin (HEP), hyaluronic acid (HA), dextran sulfate (DS), chondroitin sulfate A (CSA), chondroitin sulfate B (CSB), and chondroitin sulfate C (CSC), were chosen as target analytes. The different structures of these CAs resulted in different binding affinities with GAGs, and hence, in different output signals. Principal component analysis (PCA), LDA, and hierarchical cluster analysis (HCA) allowed for the differentiation of all six GAGs (Figure 5).

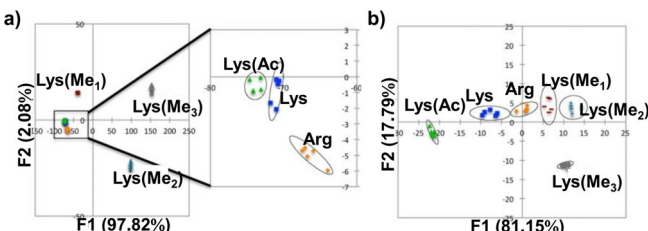


**Figure 4.** a) LDA of amino acids based on host and dye fixation and the variation of pH and solvent composition. b) LDA of amino acids based on solvent (pH, composition)/dye fixation and host variation. Reprinted with permission from ref. [84]. Copyright 2012 American Chemical Society.

#### 4.3. Supramolecular Tandem Assay (STA)

STA, proposed by Nau, can be considered as a time-resolved version of IDA.<sup>[59]</sup> In contrast to IDA, the key idea of STA is that the competitor is created but not added. STA can be used to determine the activity of enzymes in real time, requiring significant differences in binding affinities between the macrocyclic hosts and enzyme substrates/products.<sup>[86]</sup> During an enzymatic reaction, the dynamic binding of a fluorescent dye with a macrocyclic host in competition with substrate and product binding is measured (Scheme 5). The above strategy was applied to investigate the hydrolysis of Arg to ornithine catalyzed by arginase using **31** as the host and DBO as the reporter dye.<sup>[87]</sup> The corresponding association constants were obtained as 6400, 550, and 60000 M<sup>-1</sup> for Arg, ornithine, and DBO, respectively. As the affinity of Arg to **31** exceeded that of ornithine, the enzymatic reaction resulted in dye entrance into the cavity, and, hence, in a gradual switch-off of fluorescence. The same strategy was used to probe acetylcholinesterase (AChE), choline oxidase, and methyltransferase activities.<sup>[88]</sup> Additionally, Liu et al. employed STA to sense butyrylcholinesterase (BChE), a cholin-

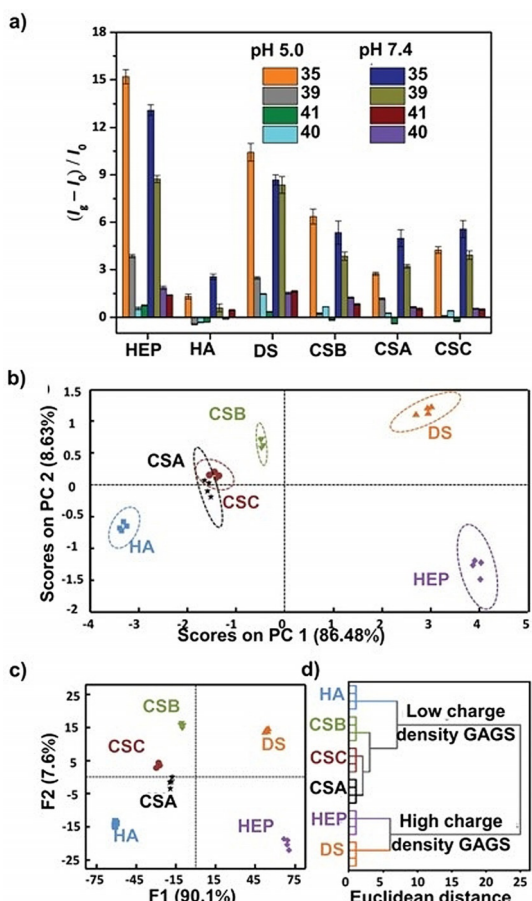
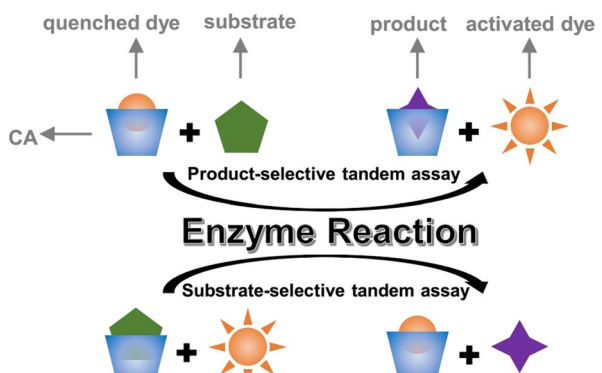


**Figure 5.** GAG discrimination via a) fluorescence recovery, b) PCA, and c) LDA. Ellipsoids on the scatter plot are drawn at 90% confidence. d) HCA dendrogram based on the Euclidean distance along with the Ward method for clustering. Reprinted with permission from ref. [85]. Copyright 2018 Royal Society of Chemistry.



**Scheme 5.** Schematic representation of STA.

esterase that always coexists with AChE in vertebrates.<sup>[89]</sup> The abnormal activity of both BChE and AChE is an indicator of some diseases. The above authors constructed a system that could generate qualitatively differentiated signals for AChE and BChE. The reporter pair was **31** + LCG, and the substrate was succinylcholine, which can be degraded by BChE but not by AChE. Fluorescence intensity

decreased upon BChE addition, but did not change in the presence of AChE (Figure 6).

In collaboration with Prof. Nau and Dr. Hennig, our group constructed a phosphorylation-responsive membrane transport system and applied it to sense the activity of protein kinase A (PKA) and protein kinase C (PKC) (Figure 7).<sup>[90]</sup> Amphiphilic CAs (**42** and **43**) were found to effectively activate the membrane transport of cell-penetrating peptides (CPPs). Then, two CPPs were designed as substrates for PKA (P1) and PKC (P2). The association constants of dephosphorylated peptides with **42** were an order of magnitude higher than those of phosphorylated peptides. These differences in binding affinities resulted in different abilities of **42** to activate peptides. Incubation of P1 with PKA decreased transport activity, and the extent of this decrease was positively correlated with incubation time and PKA concentration. The same trend was observed for PKC and P2.

Reporter pairs can also be used to monitor time-resolved changes of analyte concentration without the occurrence of a chemical reaction, as exemplified by the development of tandem membrane assaying as a versatile supramolecular

method to monitor biomembrane transport processes.<sup>[91]</sup> In this method, a membrane-impermeable reporter pair is encapsulated inside vesicles. When an analyte with a strong affinity to the host translocates into the vesicles, a time-resolved change in fluorescence due to the displacement of the dye from the host cavity is observed. This method was used by Nau et al. to investigate the diffusion of protamine through the bacterial channel outer membrane protein F (OmpF).<sup>[92]</sup> First, proteoliposomes loaded with the **31**-LCG complex were prepared. The steep increase in fluorescence observed upon the addition of protamine indicated its concentration-gradient-driven translocation into liposomes through the channel protein (Figure 8). Next, the authors incubated live cells with the **31**-LCG complex, which resulted in its spontaneous uptake.<sup>[93]</sup> Subsequent addition of bioorganic analytes having high affinities to **31** and capable of entering cells induced fluorescence turn-on. Thus, a method of detecting the uptake of bioorganic analytes by live cells was developed.

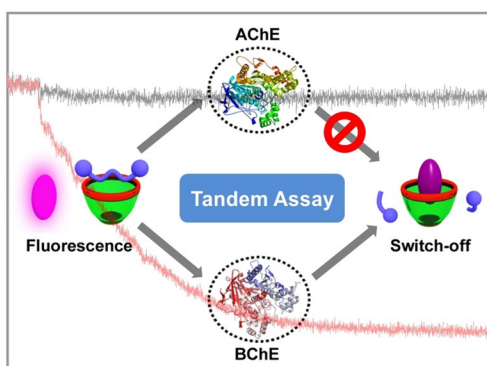


**Figure 6.** Applications of STA to specific sensing of BChE. Reprinted with permission from ref. [89]. Copyright 2013 Wiley-VCH Verlag GmbH & Co. KGaA, Weinheim.

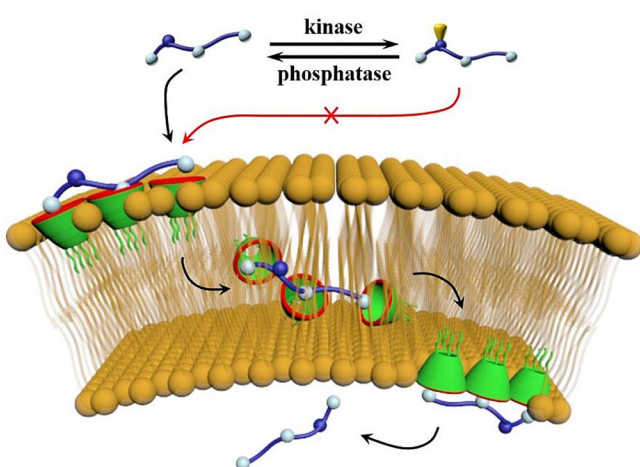


**Figure 7.** Schematic representation of phosphorylation-responsive membrane transport of peptides activated by **42** and **43**. Reprinted with permission from ref. [90]. Copyright 2017 Wiley-VCH Verlag GmbH & Co. KGaA, Weinheim.

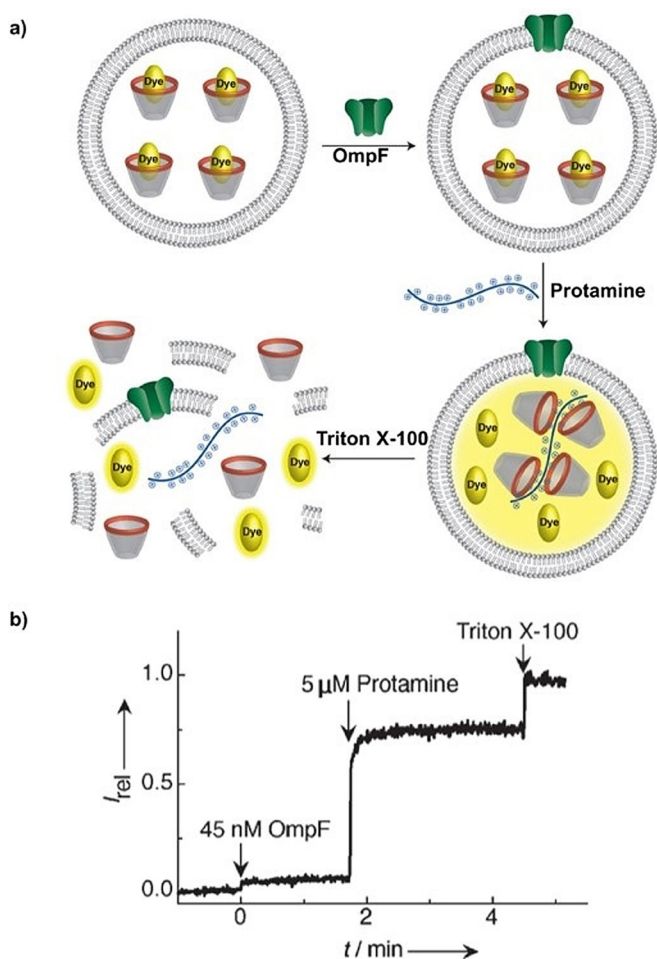


**Figure 8.** a) Schematic representation of tandem membrane assays used to monitor protamine translocation based on fluorescence measurements. b) Fluorescence intensity of **31**-LCG-loaded liposomes upon addition of OmpF, protamine, and Triton X-100. Reprinted with permission from ref. [92]. Copyright 2014 Wiley-VCH Verlag GmbH & Co. KGaA, Weinheim.

## 5. Bioimaging

Contrast agents enabling the visualization of structures inside the human body and the delineation of healthy tissues from diseased ones significantly aid clinicians in choosing the proper treatment. Therefore, numerous bioimaging approaches have been invented and used for clinical diagnosis, e.g., computed tomography, magnetic resonance imaging (MRI), positron emission tomography, single-photon emission computed tomography, optical imaging, and photo-acoustic imaging.<sup>[94]</sup> CAs find numerous applications in the field of bioimaging, mainly in optical and magnetic resonance imaging.<sup>[95]</sup>

### 5.1. Optical Imaging

Optical imaging has many prominent advantages such as sensitivity and low cost. CAs are well suited for optical imaging because they can change the spectral properties of dyes via host–guest interactions, providing a wide platform for imaging. Nau et al. employed CAs to monitor the cellular uptake of biomolecular analytes, relying on the fact that **31** can form a stable host–guest complex with LCG to quench its fluorescence.<sup>[93]</sup> Importantly, both the host and guest are biocompatible and exhibit low toxicity. Incubation of the above complex with live V79 and CHO cells resulted in its spontaneous uptake and was followed by the addition of bioorganic analytes (ACh, choline, and protamine). These analytes had high affinities to **31** and could replace LCG, causing a fluorescence switch-on response (Figure 9). The authors believed that this live-cell-based IDA provides a simple and cost-effective screening tool to monitor the uptake efficiencies of compounds that can bind CAs.

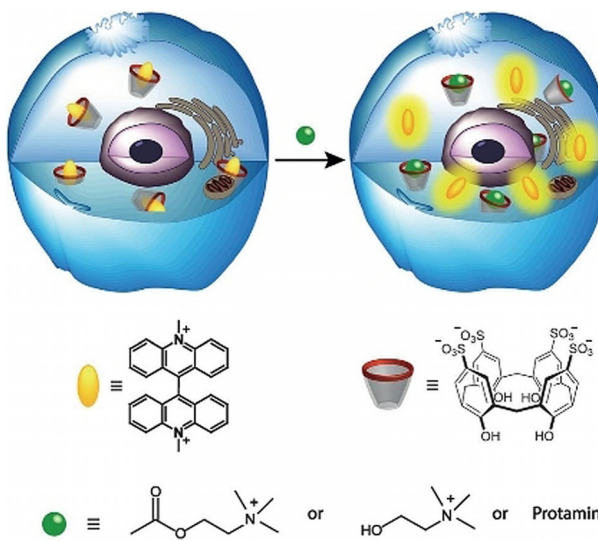


**Figure 9.** Fluorescence increase due to the uptake of analytes into cells preloaded with the **31**-LCG complex and the resulting displacement of LCG. Reprinted with permission from ref. [93]. Copyright 2015 Wiley-VCH Verlag GmbH & Co. KGaA, Weinheim.

Our group has recently reported imaging systems responsive to tumor microenvironments. Hypoxia is a central feature of many diseases including tumors and is an indicator of tumor aggression, poor prognoses, and therapeutic outcomes. An azo-group-containing CA derivative (**11**) prepared by us showed high affinity to the commercial dye rhodamine 123 (Rho123) and quenched its fluorescence.<sup>[51]</sup> In a hypoxic environment, azo groups can be reduced to release Rho123 and recover fluorescence (Figure 10). This strategy was validated through hypoxia imaging in living cells treated with the **11**-Rho123 reporter pair. Furthermore, negligible cytotoxicity was observed under experimental conditions. This noncovalent strategy based on host–guest chemistry exhibits several intrinsic advantages such as adaptability to other probes/treating agents and highly accurate release under hypoxia. Another well-known feature of tumors is biomarker overexpression. For example, the concentration of adenosine triphosphate (ATP) in tumor tissues exceeds that in normal tissues  $\approx$  10000-fold. Therefore, our group prepared a guanidinium-modified C5A pentadodecyl ether (**13**) with an extraordinarily high affinity (nm range) to commercial dyes and ATP.<sup>[53a]</sup> The binding of dyes with **13** resulted in fluorescence quenching, and the strong affinity precluded unwarranted off-target leakage during blood circulation. In tumor tissues, strong binding to ATP caused the release of dyes as well as the recovery of fluorescence. Furthermore, **13** is able to self-assemble into vesicles with a size of 115 nm, which can be used to secure the enhanced permeability and retention (EPR) effect. This strategy was summarized as biomarker displacement activation (BDA) and used for *in vivo* imaging.

Liu et al. recently reported a two-stage enhanced fluorescence method for lysosome-targeted cell imaging.<sup>[96]</sup> The synthesized dye, named ENDT, exhibited weak fluorescence emission at 625 nm, which was enhanced and red-shifted upon complexation with cucurbit[8]uril (first stage). The obtained complex assembled into nanorods, and the subsequent

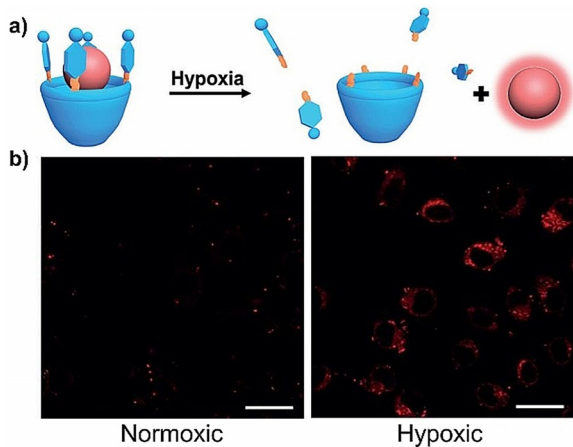


**Figure 10.** a) Schematic principles used to design noncovalent strategies for creating hypoxia-responsive systems. b) Confocal laser scanning microscopy images of A549 cells incubated with **11**-Rho123 under normoxic and hypoxic conditions for 8 h. Reprinted with permission from ref. [51]. Copyright 2019 Wiley-VCH Verlag GmbH & Co. KGaA, Weinheim.

addition of amphiphilic C4A (**43**) resulted in fluorescence enhancement (second stage) and the formation of nanoparticles (Figure 11), which were used for near-infrared lysosome-targeted cell imaging.

In addition to the cavity, the CA skeleton also contributes to optical imaging. Klymchenko et al. reported superior brightness fluorogenic nanoparticles based on the micelles of **44**.<sup>[97]</sup> These micelles were shell-cross-linked with PEGylated cyanines (Figure 12), and the size was close to that of single proteins (3–7 nm), which is ideal for cellular imaging. The CA-based nanoparticles were found to be approximately twofold brighter than quantum dots, and were applied to cell imaging, showing a distribution typical of endosomes and lysosomes. The above work provides a new principle for the development of protein-sized ultrabright fluorescent nanoparticles.



**Figure 11.** Illustration of near-infrared fluorescent supramolecular assemblies and related supramolecular aggregates. Reprinted with permission from ref. [96]. Copyright 2018 Wiley-VCH Verlag GmbH & Co. KGaA, Weinheim.

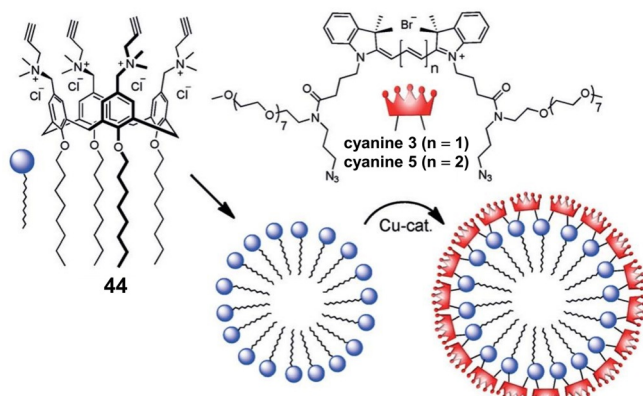


**Figure 12.** Concept of shell-crosslinking of CA micelles with a cyanine corona. Reprinted with permission from ref. [97]. Copyright 2016 Wiley-VCH Verlag GmbH & Co. KGaA, Weinheim.

## 5.2. Magnetic Resonance Imaging

MRI is one of the most important bioimaging techniques, featuring the advantages of non-invasiveness, absence of scattering or high-energy radiation, and suitability for 3D imaging. Although paramagnetic Gd<sup>III</sup> complexes are widely used as MRI contrast agents, the challenge is to prepare stable complexes that do not release toxic metal ions *in vivo*.

Casnati et al. reported a CA derivative (**45**) capable of complexing Gd<sup>III</sup> in aqueous solution.<sup>[98]</sup> The relaxivity of the corresponding complex was constant at pH 4–9, i.e., the

structure of this complex was stable in a proton concentration range spanning five orders of magnitude. Furthermore, the association constant of **45** with Gd<sup>III</sup> ( $1 \times 10^{13} \text{ M}^{-1}$ ) was sufficiently high to ensure the binding of the integrated complex to human serum albumin (HSA), which indicated that this complex can be applied as a blood-pool agent for angiography. Peters et al. reported an amphiphilic CA derivative (**46**) suitable for use as an MRI contrast agent.<sup>[99]</sup> In water, this compound formed micelles with a relaxivity about twice that of the monomer. The rotational correlation time of the monomer (390 ns) was close to the optimal value predicted for high-field contrast agents. Both the monomer and micelles were very rigid systems with negligible local contributions to the overall rotational dynamics.

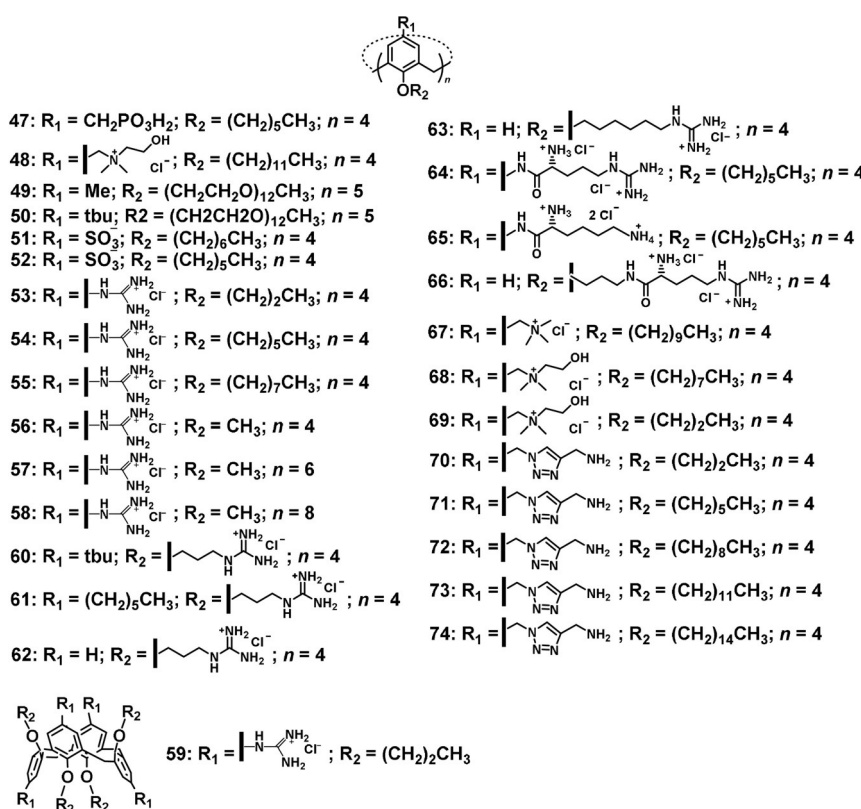
## 6. Drug Carriers

Drug delivery systems employ formulation strategies, encapsulation technologies, and/or targeted approaches to enhance the performance of drugs via (i) improving drug solubility, stability, and biocompatibility, (ii) sustainable release of drugs to change pharmacokinetics, (iii) provision of passive and/or active targeting, (iv) provision of a platform for theranostic systems, combination therapy, and controlled release.<sup>[100]</sup> To date, numerous carriers have been explored for drug delivery, e.g., liposomes, polymers, dendrimers, gold nanoparticles, and proteins.<sup>[100,101]</sup> As drug carriers, CAs offer the advantages of well-defined molecular structures with precise sizes and determined molecular weights, host–guest recognition sites and various drug loading sites, amphiphilicity for controllable assembly, and ease of targeting and response group modification. Consequently, numerous CA-based drug delivery systems have been reported and broadly categorized as those featuring drug loading within the cavity, drug loading within the assembling regions, and CAs containing nanovalves for controlled release (Scheme 7).

### 6.1. Drug Loading within the Cavity

Noncovalent encapsulation of drugs into CA cavities has been widely used to improve drug properties (e.g. solubility and stability) and/or realize drug delivery.<sup>[102]</sup> Menon et al. reported the complexation of **1** and **2** with carvedilol (CDL), a poorly water-soluble drug, revealing that this complexation greatly increased CDL solubility and demonstrating a linear relationship between CDL solubility in water and CA concentration.<sup>[103]</sup>

Amphiphilic CAs can self-assemble as nanoparticles and act as drug nanocarriers. Raston et al. reported that vesicles formed by amphiphilic phosphonomethyl C4A (**47** in Scheme 6) effectively bind carboplatin and increase its anticancer efficacy.<sup>[104]</sup> The host–guest vesicles were relatively stable at pH 7.4, with  $\approx 20\%$  of loaded carboplatin released after two days at 37°C, while at pH 5.5, the above release was accomplished within 5 h. This difference was explained by considering the  $pK_a$  of phosphonic acid head groups (7.2): protonation at pH 5.5 decreased polarity and destabilized



Scheme 6. Molecular structures of CAs (47–74) mentioned in this Review.

vesicles. Cell assays showed that the introduction of CA vesicles increased the efficacy of carboplatin toward ovarian cancer cells 4.5-fold, lowered  $\text{IC}_{50}$  10-fold, and markedly increased the percentage of cells in the S-phase (DNA replication) of the cell cycle. Our group has realized activatable photodynamic therapy (PDT) based on the BDA strategy (Figure 13).<sup>[53a]</sup> The clinical usage of PDT is hindered by its unexpected dark toxicity due to the “always-on” model and low tumor specificity. In our strategy, a photosensitizer (PS) was preloaded into the receptor cavity (**13**), with the photoactivity and fluorescence completely annihilated and released by overexpressed biomarkers (ATP) in tumor tissues. The above system was successfully used for tumor imaging and targeted therapy *in vivo*, paving a new avenue for theranostics. The BDA strategy has several advantages, e.g., the employment of approved PSs, adaptability to different PSs, and traceless release of PSs with high fidelity. As a follow-up to this work, our group developed a tandem stimuli-responsive assembly based on **35** and Eosin Y (a kind of PS)-modified hyaluronic acid, which exhibited hyaluronidase-triggered disassembly and ATP-activated release of Eosin Y, which is thus potentially suited for precision delivery with respect to tumor phototheranostics.<sup>[105]</sup>

In addition to being loaded in cavities at the periphery of assemblies, drugs can also be loaded in cavities at the assembly core. Zhou et al. developed a PS delivery system based on the self-assembly of PEGylated C4A (**14**). The grafted PEG arms endowed CA with solubility in the aqueous phase, and binding with PSs resulted in the formation of

supramolecular amphiphiles that self-assembled into supramolecular polymeric micelles (Figure 14).<sup>[53b]</sup> The encapsulation of PSs into CAs avoided the aggregation of PSs and fluorescence self-quenching. Chlorin e6 (Ce6) was employed as a hydrophobic model PS in this work. Micelles formed by **14**-Ce6 had a diameter of  $\approx 100$  nm and could be preferentially delivered into tumors because of the EPR effect. In vitro experiments showed that **14** had low cytotoxicity and that **14**-Ce6 exhibited higher PDT efficacy than free Ce6.

## 6.2. Drug Loading within Assembling Regions

In the case of assemblies, in addition to being loaded in cavities, drugs can also be loaded within the assembling regions (Scheme 7d–f).<sup>[100,102g,106]</sup> Chen et al. developed a vehicle for the *in vivo* delivery of curcumin using **47**, showing that **47** self-assembled into micelles (average size = 3.86 nm) with high curcumin encapsulation efficiency.<sup>[107]</sup> Cell culture experiments suggested that these micelles could sustainably release curcumin in a pH-dependent manner and inhibited the proliferation, invasion, migration, and tumor spheroid formation of BT-549 cells more efficiently than the free drug. This enhanced performance was ascribed to the fact that micelles

minimized the pH-dependent aggregation of curcumin and inhibited the proliferation, invasion, migration, and tumor spheroid formation of BT-549 cells more efficiently than the free drug. This enhanced performance was ascribed to the fact that micelles

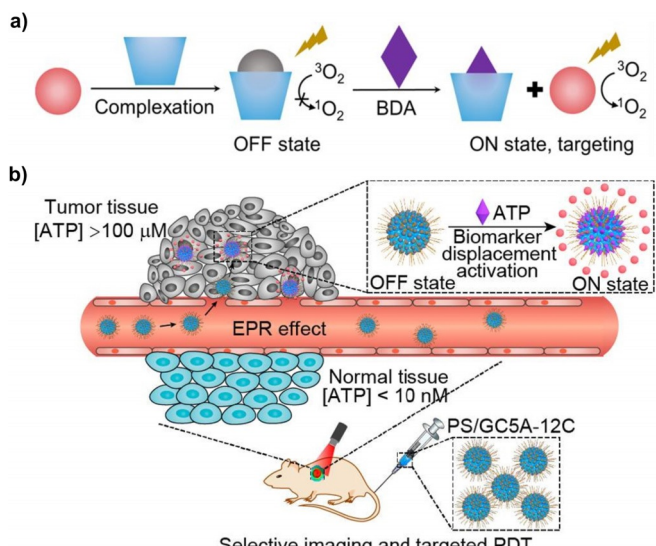
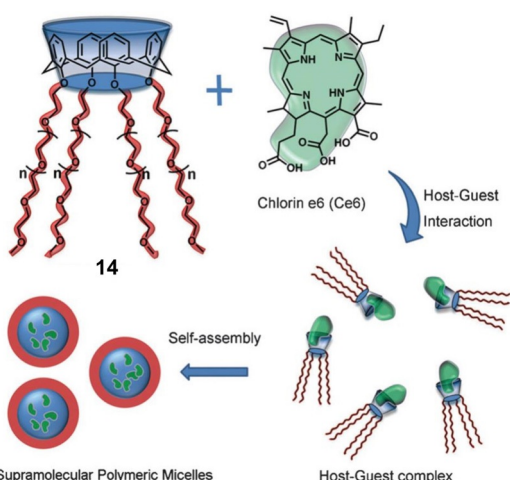
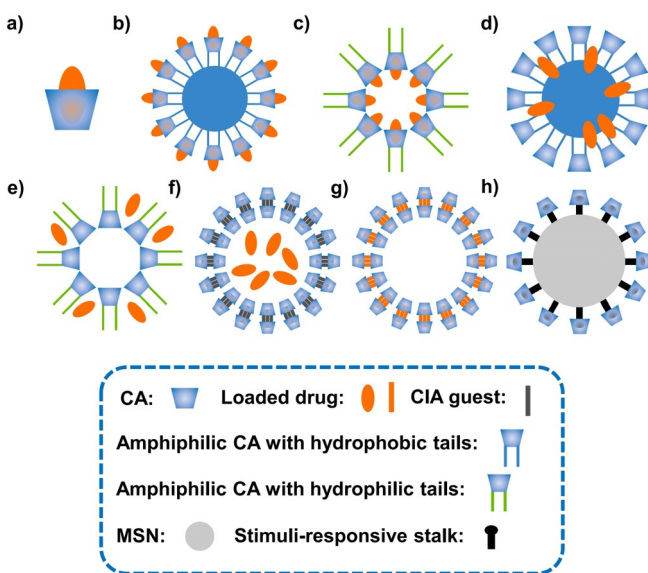


Figure 13. a) Proposed host-guest strategy, BDA. b) Schematic illustration of tumor-selective imaging and targeted PDT performed on tumor-bearing mice with dual selectivity arising from the EPR effect of the nanocarrier and tumor-ATP response. Reprinted with permission from ref. [53a]. Copyright 2018 American Chemical Society.



**Figure 14.** Formation of supramolecular polymeric micelles from **14** and Ce6 based on host–guest interactions. Reprinted with permission from ref. [53b]. Copyright 2011 Royal Society of Chemistry.



**Scheme 7.** Schematic illustration of CA-based drug delivery systems.

were taken up by pinocytosis and acted as a curcumin depot inside cells to prevent the precipitation of this drug. The enhancement of drug solubility, eye surface permanence, and penetrability is a topic attracting much attention. Consolini et al. developed potential eye drops by entrapping curcumin in a choline-modified C4A (**48**)-based nanoaggregate.<sup>[108]</sup> Choline is an alkoxyamine that is well tolerated by the eye and can cross the cornea via low-affinity facilitated diffusion. The positive charge of choline can electrostatically interact with the negatively charged ocular surface and mucus. Aggregation successfully enhanced the solubility (9000-fold) and stability (7.5-fold) of curcumin. The effects of curcumin on inflammation and oxidative biomarkers was also improved via the formation of **48** nanoaggregates. The same trend was also observed in vivo, indicating the high potential of this system for ophthalmic applications.

Drugs can be loaded both in hydrophobic and hydrophilic tails. Notti et al. reported the assembly of PEGylated C5A (**49** and **50**) to afford drug carriers.<sup>[109]</sup> Rose Bengal (RB), which is used in ophthalmology for the diagnosis of dry eyes, was encapsulated in the corresponding micelles, which successfully improved RB lipophilicity and enhanced its capacity to cross biological barriers such as cell membranes.

In addition to the traditional amphiphilic assembly, CAs can also be assembled into supra-amphiphiles for drug delivery. In 2012, Liu et al. developed a cholinesterase-responsive drug delivery system, employing **31** and enzyme-cleavable myristoylcholine to form binary vesicles that were highly specifically and efficiently dissipated by cholinesterase.<sup>[110]</sup> The validity of enzyme-responsive release was confirmed by trapping a fluorescence dye inside vesicles as a beacon. As both myristoylcholine and myristic acid (enzymatic reaction product) form micelles, myristoylcholine itself could not realize the release of loaded drugs, which indicated the significance of **31** (Figure 15). In view of the fact that cholinesterase is a key protein overexpressed in patients with Alzheimer's disease, the above system has potential for the delivery of related drugs. Liu et al. also developed another enzyme-responsive drug delivery system, employing **31** to bind protamine (as an enzyme-cleavable guest) and form binary vesicles.<sup>[111]</sup> In the presence of serine protease trypsin, protamine was converted to amino acids and peptides, promoting the rupture of vesicles and the release of drugs encapsulated therein. The system featured high selectivity, i.e., other enzymes such as Exo I could not cause drug release.

CAs can also induce the assembly of drugs into nanostructures, usually with a high drug loading efficiency (Scheme 7g). In 2014, Liu et al. employed **31** and **51** to assemble the small-molecule antipsychotic drug chlorpromazine into nanostructures with loading efficiencies of 61 and 46%, respectively.<sup>[112]</sup> The presence of the host–guest recognition sites of **51** on the outer layer surface allowed a targeting agent, trimethylated chitosan, to be further noncovalently anchored onto nanoparticles. In 2015, the above authors proposed a “drug chaperone” concept.<sup>[113]</sup> Specifically, two

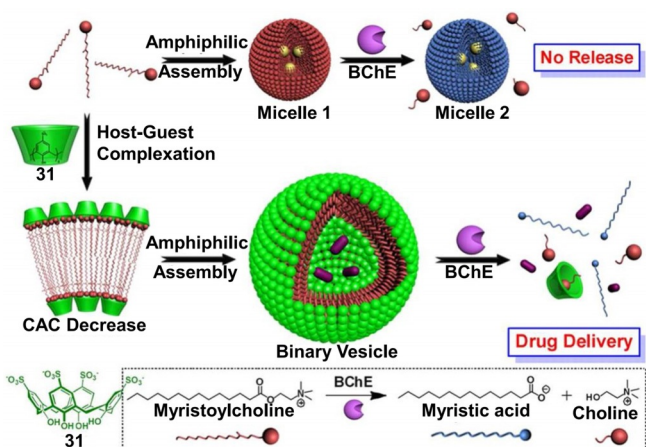


**Figure 15.** Schematic illustration of amphiphilic assemblies of myristoylcholine in the absence and presence of **31**. Reprinted with permission from ref. [110]. Copyright 2012 American Chemical Society.

drugs (Irinotecan and Mitoxantrone) were directly co-assembled with an amphiphilic CA (**52**), and the targeting ligands, biotin-pyridinium and hyaluronic acid-pyridinium, were appended at the nanoparticle surface via host-guest interactions. Cell experiments showed that the anticancer activities of free drugs improved after co-assembly with CAs and further functionalization with targeting ligands.

### 6.3. CA-Containing Nanovalves for Controlled Release

A nanovalve is a molecular machine fabricated by combining a movable part with a covalent attachment to a solid nanoparticle supported at the pore opening.<sup>[114]</sup> In view of their controllable recognition ability, macrocycles (including CAs) are widely used as nanovalve components (Scheme 7h). Yang et al. developed a series of functionalized mesoporous silica nanoparticles (MSNs) based on CAs for drug delivery, including an enzyme-responsive system,<sup>[115]</sup> and an ACh-responsive system.<sup>[116]</sup> In 2016, they developed dual-responsive MSNs based on **31** and **32**.<sup>[117]</sup> These MSNs were functionalized with cleavable disulfide-bond-containing alkylammonium stalks and encircled by CAs. The presence of CAs reduced premature cargo release. Cargo was efficiently released either in response to L-glutathione (GSH), via cleavage of disulfide bonds in the stalks, or in response to pH variation, via reduction of the CA-MSN binding affinity (Figure 16).

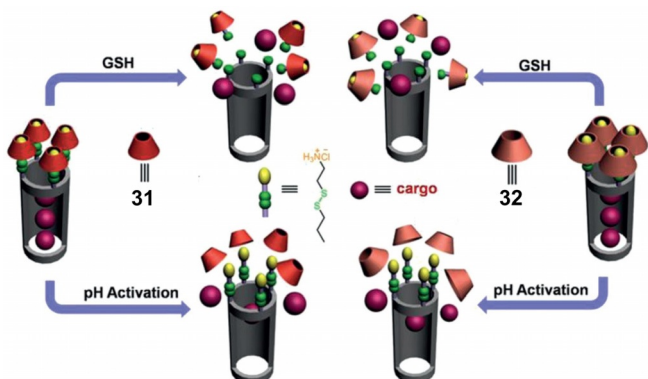


**Figure 16.** Illustration of the controlled release of cargo from stimuli-responsive supramolecular nanovalves based on MSNs. Reprinted with permission from ref. [117]. Copyright 2015 Wiley-VCH Verlag GmbH & Co. KGaA, Weinheim.

### 7. Gene Delivery and Transfection

Gene delivery, i.e., the introduction of foreign DNA or RNA into host cells, is important for both fundamental research and biomedical applications.<sup>[118]</sup> Naked DNA and RNA exhibit very poor capacity to transfect cells because of the presence of barriers and low stability.<sup>[119]</sup> Therefore, efficient gene delivery requires the use of specially designed nucleic acid vehicles. A number of viral vectors have successfully progressed to clinical trials and even to the

market.<sup>[120]</sup> However, as their widespread applications are limited by intrinsic immunogenicity and high production costs, numerous nonviral vectors such as lipids, polymers, dendrimers, and macrocycles have been designed.<sup>[121]</sup> Macrocycles are an emerging class of molecules for this application, featuring persistent shapes and thus allowing for a higher level of supramolecular organization of DNA complexes.<sup>[122]</sup> As the third generation of macrocyclic hosts, numerous CAs are capable of binding DNA,<sup>[123]</sup> and some of them have been used to detect mismatch<sup>[124]</sup> and hybridization.<sup>[125]</sup> Some CAs are able to denature DNA by complexation and can therefore be used to develop antibacterial and/or anticancer drugs.<sup>[126]</sup> Importantly, certain CAs exhibit transfection ability, especially those modified with guanidinium, tetraalkylammonium, and amino groups.<sup>[121d, 127]</sup>

Ungaro et al. anchored guanidinium groups at the upper or lower rim of CAs (**53–63**) and investigated the dependence of DNA condensation and cell transfection properties on macrocycle lipophilicity, size, conformation, and spacer length.<sup>[128]</sup> DNA pEGFP-C1 (encoding green fluorescence protein) was employed in these experiments, and the results showed that attachment of guanidinium groups at the lower rim significantly enhanced cell transfection ability and reduced toxicity. When the most efficient compound (**62**) was formulated with a helper lipid, 1,2-dioleoyl-sn-glycero-3-phosphoethanolamine (DOPE), the achieved transfection efficiency exceeded that of commercially available lipofectamine LTX (Figure 17a,b). In 2013, the same team synthe-

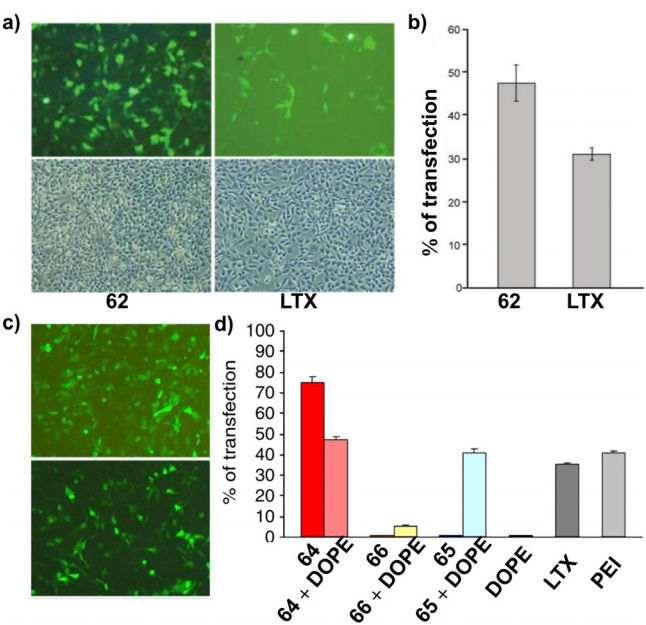


**Figure 17.** a) Fluorescence microscopy images (top) and phase-contrast images (bottom) of human Rhabdomyosarcoma cells transfected (in green) by treatment with pEGFP-C1 plasmid and **62**/DOPE formulation. b) In vitro transfection efficiencies (percentage of cells transfected upon treatment) of **62**/DOPE and LTX. Reprinted with permission from ref. [128c]. Copyright 2012 American Chemical Society. c) Fluorescence microscopy images of human Rhabdomyosarcoma cells transfected (in green) by treatment with pEGFP-C1 plasmid formulated with **64** (top) and LTX (bottom). d) In-vitro transfection efficiency as percentage of transfected cells. Reprinted with permission from ref. [129]. Copyright 2013 Springer Nature.

sized Arg- and Lys-modified CAs (**64–66**) and compared their transfection efficiencies in the absence and presence of DOPE with those of LTX and polyethyleneimine (PEI) (Figure 17c,d).<sup>[129]</sup> Among these species, **65** showed the highest efficiency.

Junquera et al. constructed lipoplexes using the amphiphilic tetraalkylammonium-modified C4A (**67**), DOPE, and DNA pEGFP-C3.<sup>[130]</sup> The transfection efficiency of **67**/DOPE-pDNA lipoplexes was evaluated by measuring the GFP expression level in HEK293T cells by fluorescence microscopy. The best transfection performance was observed at a fraction of **67** of 0.2 and an effective charge ratio of 20.<sup>[130]</sup> Klymchenko et al. synthesized a choline-modified amphiphilic C4A (**68**) that could self-assemble into 6-nm-diameter micelles and deliver DNA.<sup>[131]</sup> The addition of DNA caused aggregation and an increase of micelle diameter to 50 nm (Figure 18). These nanoparticles showed high gene transfection efficiencies in cell cultures, while poorer performance was observed for a shorter-tail CA (**69**).

Sakurai studied the transfection efficiency of amino-modified C4A-based lipids with different alkyl chain lengths (C3–C15, **70–74**), revealing that **71** lipoplexes exhibited the highest efficiency, **73** and **74** lipoplexes featured slightly lower efficiencies, while **70** and **74** lipoplexes were not active.<sup>[132]</sup>

The **71**, **72**, and **73** lipoplexes also exhibited low cytotoxicity.

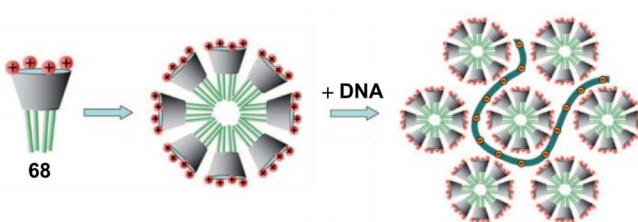


**Figure 18.** Simplified self-assembly of amphiphilic **68** into micelles and further DNA complex formation. Reprinted with permission from ref. [131]. Copyright 2011 Wiley-VCH Verlag GmbH & Co. KGaA, Weinheim.

## 8. Therapeutic Agents

In addition to being applied as pharmaceutical excipients, macrocycles themselves can also be used as therapeutic agents, generating the concept of macrocyclic therapeutics. Macrocylic molecules, which do not carry any encapsulated or covalently linked pharmaceutical agents, can show biomedical activities. For example, CDs can be applied as neuromuscular block antidotes, regulators of cholesterol metabolism, anti-infective agents, and antitoxins.<sup>[5,133]</sup> Moreover, cucurbiturils and pillararenes can be used to treat paraquat poisoning.<sup>[134]</sup> The ease of CA modification has resulted in the generation of a large corresponding material library, and many CA derivatives have greatly promoted the development of macrocyclic therapeutics.<sup>[135]</sup>

### 8.1. Antibacterial, Antifungal, and Antiviral Properties

Numerous CAs have been reported to exhibit antibacterial and/or antifungal activities.<sup>[136]</sup> The abundance of available substituents endows CAs with a variety ways to kill bacteria/fungi, e.g., via membrane disorganization, DNA damage, and inhibition of DNA replication. The structures, bioactivities, and action modes of CAs are summarized in Table 1.

Conditions related to infection with the human immunodeficiency virus (HIV) cause numerous deaths every year. Regnouf-de-Vains et al. synthesized nine C4A derivatives (**31**, **113–120**; Scheme 8) and studied their anti-HIV properties and cytotoxicity.<sup>[150]</sup> Most of these compounds had antiviral activities of 10–50  $\mu$ M, while no cytotoxicity was observed at concentrations up to 100  $\mu$ M. Hamilton et al. synthesized a series of C4A derivatives (**121–131**) and studied their abilities to inhibit HIV and hepatitis C virus (HCV) infections, showing that the introduction of lower-rim alkylation to maintain the cone conformation is important for potent dual antiviral activity.<sup>[151]</sup> In addition, aromatic isophthalate spacers at the upper rim were essential for anti-HIV activities, and diacid groups were necessary for anti-HCV effects.

In addition, CAs can also inhibit HIV by regulating the related proteins. Luo et al. designed a series of C4A-based  $\beta$ -diketo derivatives (**132–140**) as novel HIV-1 integrase inhibitors with stand transfer inhibition IC<sub>50</sub> values of 5.9–21.2  $\mu$ M.<sup>[152]</sup> The molecular docking results for **134** and **139** suggested that the macrocyclic skeletons of C4A bind to the hydrophobic cavity in the prototypic foamy virus integrase active site (Figure 19). Mannosylated CA derivatives were reported to interact with lectins and act as inhibitors.<sup>[153]</sup> Sansone et al. synthesized four mannosylated CAs (**141–144**) and studied their properties as dendritic cell-specific ICAM-3 grabbing non-integrin (DC-SIGN) binding inhibitors.<sup>[154]</sup> HIV exploits the interaction between the mannose-rich structures of its envelope glycoprotein gp120 and DC-SIGN to be transported toward T-cells and infect them. The above authors used a mannosylated BSA as a model of HIV gp120 and evaluated the capability of CAs to inhibit binding

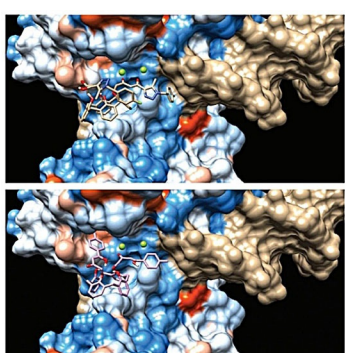


**Figure 19.** Best docking positions of **134** (gold, top) and **139** (light purple sticks, bottom) in the active site of PFV IN. Mg<sup>2+</sup> is represented by a green ball. Color by atom type: purple and gray, C; blue, N; green, F; red, O. Reprinted with permission from ref. [152]. Copyright 2015 Wiley-VCH Verlag GmbH & Co. KGaA, Weinheim.

**Table 1:** Antibacterial and/or antifungal activities of CA derivatives and the corresponding mechanisms. N.M. = not mentioned, N.D. = not detected, G.N. = Gram negative, G.P. = Gram positive. The structures of corresponding CAs (75–112) are shown in Scheme 8.

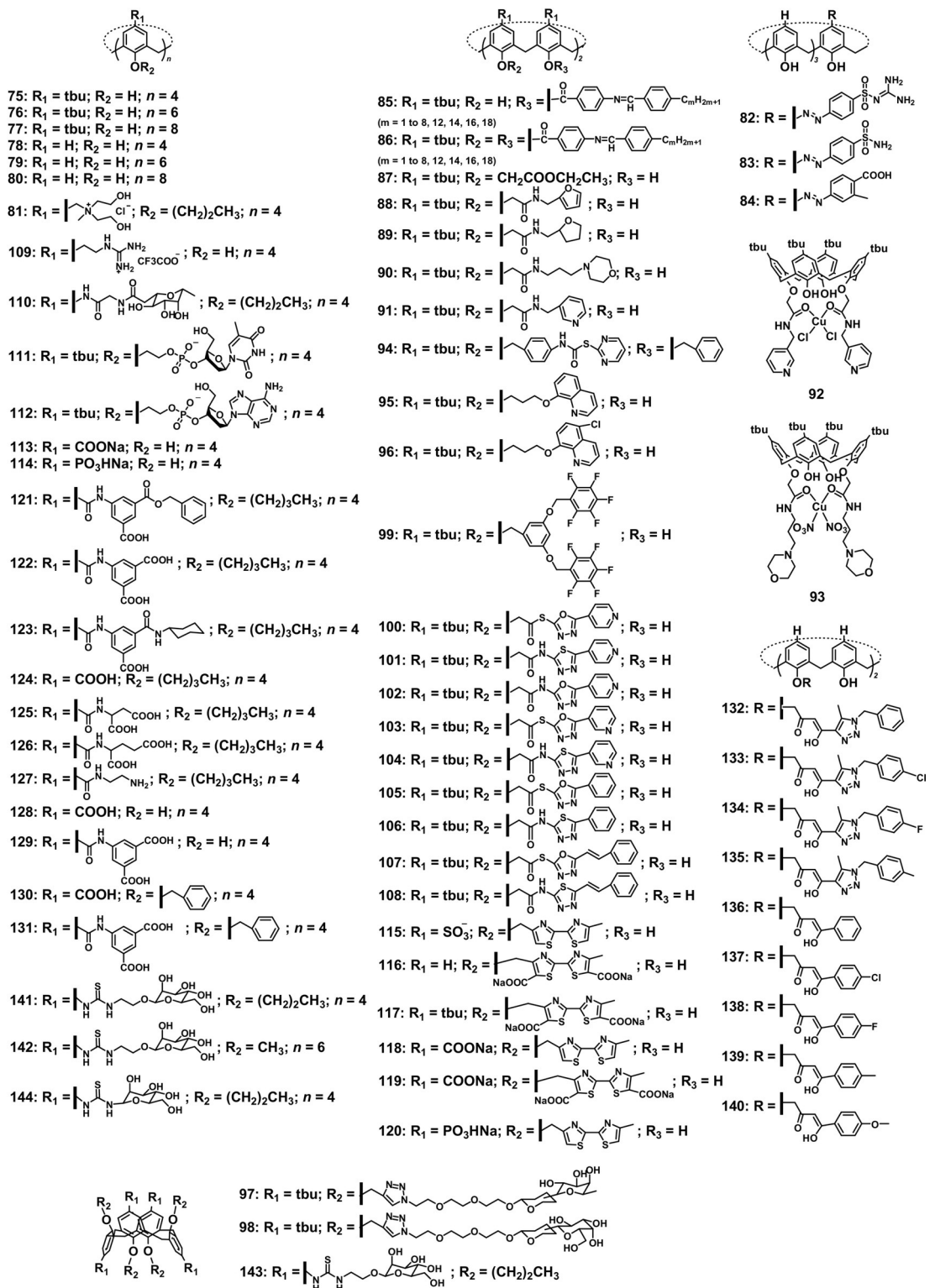
CA	Antibacterial activity	MIC ( $\mu\text{g mL}^{-1}$ )	Antifungal activity	MIC ( $\mu\text{g mL}^{-1}$ )	Mechanism	Ref.
75–80	N.M.	–	<i>Parascosporidium</i>	mostly 16–128	N.M.	[137]
81	G.N.	4	N.M.	–	disorganization of bacterial membrane	[138]
82–84	G.P.	0.97–62.5	no activity	—	inhibition of microbial enzymes	[139]
85 and 86	G.P.	mostly $\approx 100$	<i>C. albicans</i>	$\geq 200$	N.M.	[140]
87–91	G.P. and G.N.	39–10 000	<i>C. albicans</i> , <i>C. tropicalis</i>	2500–10 000	DNA damage, DNA replication inhibition	[141]
92 and 93	G.P. and G.N.	N.D.	<i>C. albicans</i> , <i>C. tropicalis</i>	N.D.	DNA damage, DNA replication inhibition	[141]
94	<i>Salmonella typhimurium</i> NRRLB 4420, <i>Bacillus cereus</i> ATCC 11778, <i>Staphylococcus aureus</i> NRRL B767, and <i>Bacillus subtilis</i> NRS 744	N.M.	<i>C. albicans</i>	N.M.	N.M.	[142]
95 and 96	N.M.	–	<i>C. albicans</i>	N.M.	N.M.	[143]
97 and 98	<i>Pseudomonas aeruginosa</i>	N.M.	N.M.	–	inhibition of <i>Pseudomonas aeruginosa</i> aggregation, biofilm formation, adhesion on epithelial cells, and destruction of alveolar tissues	[144]
12, 68, 69	<i>S. aureus</i> ATCC 29213, <i>E. coli</i> ATCC 25922	16–32	N.M.	–	interaction with cell membrane, change intracellular osmotic environment of bacteria	[52]
99	better for G.P.	N.M.	N.M.	–	inhibition of oxidative metabolism	[145]
100–108	G.P. and G.N.	100–250	<i>C. albicans</i> , <i>A. clavatus</i>	100–500	N.M.	[146]
109	G.P. and G.N.	4–64	N.M.	–	disorganization of bacterial membrane	[147]
110	<i>P. aeruginosa</i>	N.M.	N.M.	–	inhibition of biofilm formation	[148]
111, 112	<i>Penicillium digitatum</i>	N.M.	N.M.	–	inhibition of DNA replication	[149]

between DC-SIGN and the mannosylated BSA by SPR. In contrast to **143**, which was not soluble, the other three CAs featured IC<sub>50</sub> values in the  $\mu\text{M}$  range, with the best performance observed for **141** (206.6  $\mu\text{M}$ ).

## 8.2. Anticancer Properties

CAs have been widely applied as anticancer agents, mainly acting as DNA synthesis inhibitors, angiogenesis antagonists, oncogene suppressors, and upregulators of tumor suppressor genes.<sup>[55,155]</sup>

Yan et al. prepared a series of CnA ( $n=4, 6$ , and  $8$ ) polyhydroxyamine derivatives (**145–157** in Scheme 9) and studied their antitumor activities using six cancer cell lines.<sup>[156]</sup> The IC<sub>50</sub> values of **145–148** ranged from 1.6 to 11.3  $\mu\text{M}$ . Cell cycle analysis showed that exposure of SKOV3 cells to **145** induced cell cycle arrest in the G0/G1 phase, indicating DNA synthesis inhibition. Neri et al. reported several C4A conjugates (**158–162**) with anticancer properties that could intercalate into the DNA minor groove, as revealed by docking and circular dichroism studies (Figure 20).<sup>[157]</sup> Three human tumor cell lines were employed to evaluate the in vitro

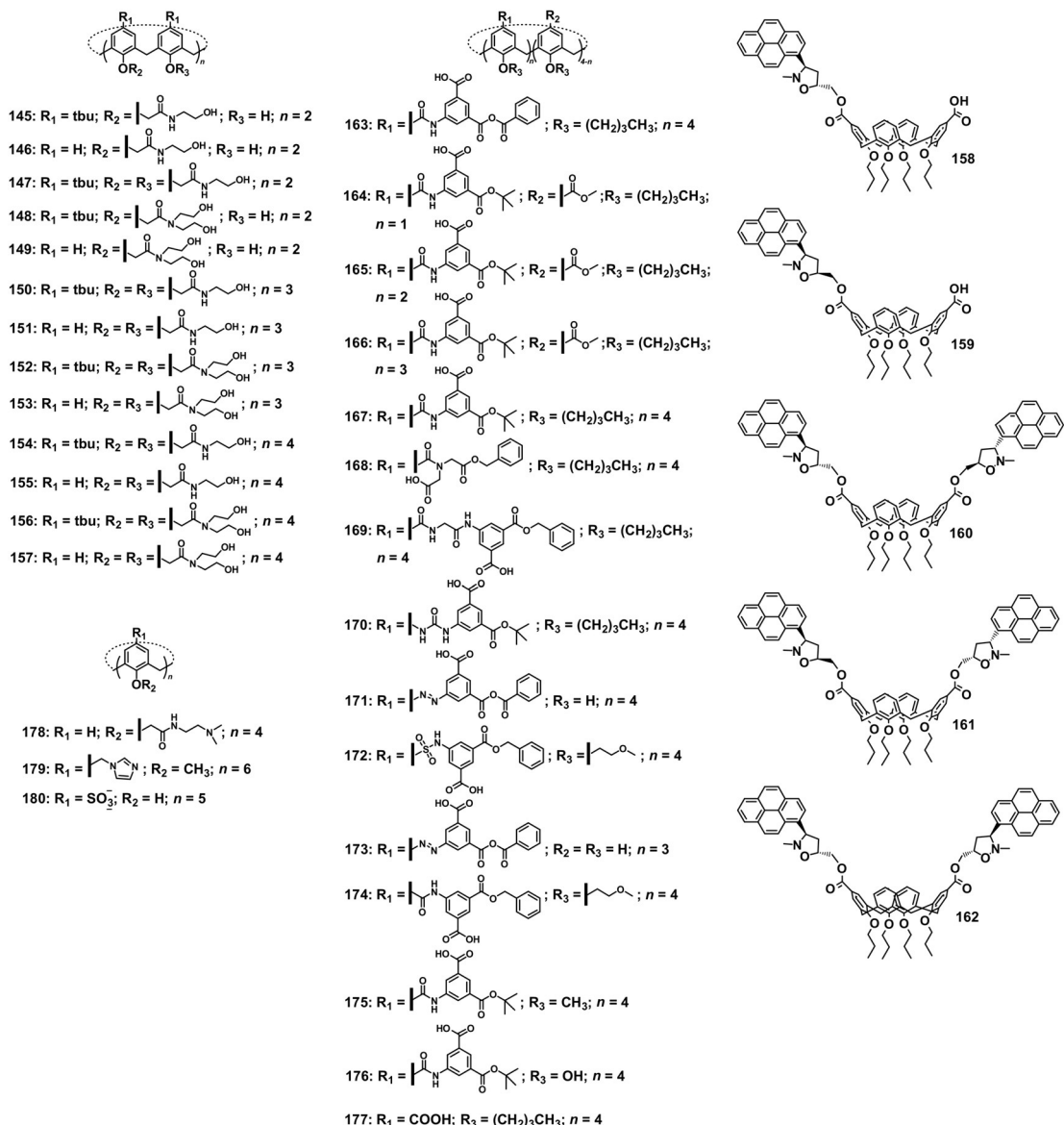


**Scheme 8.** Molecular structures of CAs (75–144) mentioned in this Review.

cytotoxicity of the above species, with the most potent one exhibiting an IC<sub>50</sub> of 95 nm.

Hamilton et al. reported a series of potent C4A-based platelet-derived growth factor (PDGF) antagonists (**163–177**) able to inhibit PDGF-stimulated PDGF receptor (PDGFR)

tyrosine phosphorylation.<sup>[158]</sup> CAs were designed to bind to the three-loop region of PDGF and disrupt its interaction with PDGFR. As both PDGF and PDGFR are required for tumor growth and angiogenesis, the disruption of their interaction resulted in tumor starvation and growth reduction. CAs with



Scheme 9. Molecular structures of CAs (145–180) mentioned in this Review.

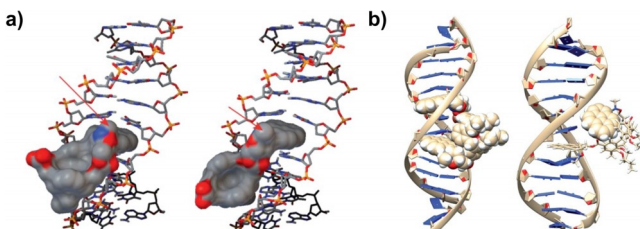


Figure 20. a) Plots representing 158 (left) and 159 (right) intercalated into the  $(\text{dA-dT})_2$  dodecamer of the minor groove. Red arrows indicate the  $\text{N-Me}$  group of the isoxazolidine ring. b) Plot representing 161 intercalated into the  $(\text{dA-dT})_2$  dodecamer of the major groove. After 1 ns of molecular dynamics simulation, the two pyrene moieties were both intercalated (left); after 5 ns, only one pyrene moiety was intercalated, and the other was completely deintercalated, and the corresponding pocket was closed (right). Reprinted with permission from ref. [157]. Copyright 2014 Wiley-VCH Verlag GmbH & Co. KGaA, Weinheim.

diazoo, amide, and glycine linkers (163, 169, 171) had satisfactory activities, while those with sulfonamide and urea linkers (170, 172) had low activities. Alkylation at the lower rim was found to be unnecessary. Compound 178, a CA derivative with anticancer activity, is currently undergoing a phase-I clinical trial. In 2006, Mayo et al. reported that 178 can inhibit angiogenesis and features  $\text{IC}_{50}$  values as low as  $2 \mu\text{M}$ .<sup>[159]</sup> According to the suggested working principle, 178 can bind to galectin-1, a carbohydrate-binding protein related to cancer cell proliferation, and suppress its activity.<sup>[160]</sup> Compound 178 also showed synergy with several cytotoxic and targeted therapies when administered first.<sup>[160b]</sup> Moreover, the favorable pharmacokinetics (PK) of 178 promoted its application in clinical therapy.<sup>[161]</sup>

Sakaguchi et al. reported that C6A derivatives bearing six imidazole groups (179) enhanced the transcriptional activity of a mutant p53 tumor suppressor protein.<sup>[162]</sup> The mutation of

the *TP53* gene, which encodes the p53 protein, causes multiple tumors because of the destabilization of the tetrameric structure of p53. Thermal denaturation curves showed that **179** could stabilize the p53 structure under physiological conditions. Furthermore, cellular experiments demonstrated that **179** also enhanced the transcriptional activity of p53. C6A (**80**) was reported to decrease the aggressiveness of a drug-resistant human pancreas carcinoma cell line, leading to cell cycle arrest in the G0/G1 phase by downregulation of PIM1 (proviral integration site for the moloney murine leukemia virus), CDK2 (cyclin-dependent kinase), CDK4, and retinoblastoma proteins.<sup>[163]</sup> The signal transduction of Mer (tyrosine-protein kinase receptor) and AXL (tyrosine-protein kinase receptor UFO), both of which are usually overexpressed in pancreatic cancer, was also abolished by **80**. The proteins positively modulated by Mer and AXL were also found to be suppressed. These findings highlight that **80** can be used to overcome pancreatic cancer aggressiveness.

### 8.3. Detoxification

Liu et al. reported that **180** can potentially be used for the clinical treatment of viologen poisoning because of its strong affinities to viologens, as exemplified by mice tests on paraquat (PQ), a typical viologen.<sup>[164]</sup> The results showed that **180** significantly reduced the mortality of poisoned mice. Complexation between **180** and PQ complicated the interaction of the latter with reducing agents in cells and the generation of radical cations. In addition, **180** could deactivate radicals and bind transition metal ions catalyzing the generation of HO<sup>·</sup> (Figure 21). More importantly, when **180** was administered 1 h later than PQ, no mortality was observed, as the biodistribution of **180** in blood is achieved faster than that of PQ, which gives patients time to seek medical help. Subsequently, Qi et al. studied the *in vivo* PK of PQ detoxification by **31**.<sup>[165]</sup>

Succinylcholine (Sch) is the only depolarizing neuromuscular blocking agent. However, this compound exhibits numerous side effects such as myalgia and prolonged apnea.<sup>[166]</sup> Wang et al. used supramolecular therapeutics to treat these side effects, employing **31**, which exhibited strong affinities to Sch. In an Sch-overdosed mouse model, **31** was injected immediately after Sch administration. The overall survival rates significantly increased, indicating successful detoxification.

### 8.4. Inhibition of Amyloid Fibrillation

As CAs can interact with a variety of proteins, it is not surprising that they can also regulate the structures and functions of these proteins. For example, sol-gel encapsulation of lipase in the presence of CA derivatives enhances its activity and enantioselectivity.<sup>[167]</sup> Aminophosphonic acid modified C4A was reported to inhibit the activity of alkaline phosphatase,<sup>[168]</sup> with numerous other examples available.<sup>[169]</sup> Herein, we only introduce reports describing how CAs inhibit amyloid fibrillation, which is related to a wide range of

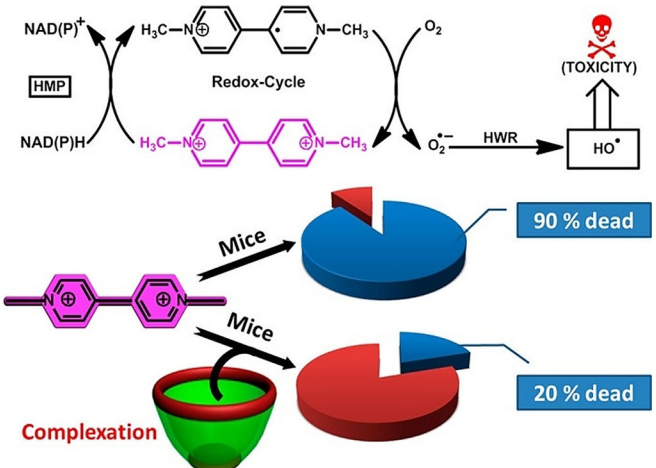


**Figure 21.** Mechanism of PQ toxicity and the application of **180** for supramolecular detoxification. Reprinted with permission from ref. [164]. Copyright 2009 American Chemical Society.

diseases such as Alzheimer's disease, Parkinson's disease, and type II diabetes.

The amyloid state of a protein is a highly ordered aggregate in which the polypeptide chains adopt a fibrillar structure. Sun et al. reported that **31**, **32**, and **33** effectively delayed the fibrillation of amyloid- $\beta$  (A $\beta$ <sub>42</sub>), which is the hallmark of Alzheimer's disease, and exhibited reduced cytotoxicity (Figure 22).<sup>[170]</sup> These CAs bound A $\beta$ <sub>42</sub> with association constants of the order of 10<sup>3</sup> M<sup>-1</sup>, and their effectiveness was determined to be in the order of **33** > **32** > **31** according to thioflavin T (ThT, a dye interacting with fibers and exhibiting fluorescence) assays. The higher efficiency of **33** was ascribed to its larger and more flexible cone, which resulted in stronger interactions with A $\beta$ <sub>42</sub> than in the case of **31** and **32**.

Our group recently co-assembled an amphiphilic CA (**18**) with an amphiphilic CD to efficiently inhibit amyloid fibrillation (Figure 23).<sup>[53c]</sup> A $\beta$ <sub>42</sub> contains two lysines, which can strongly bind to **18**, and one tyrosine, which is an ideal

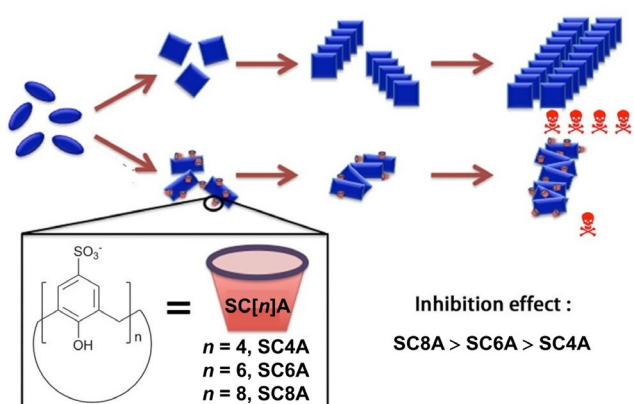


**Figure 22.** Schematic representation of amyloid aggregation inhibition by CAs. Reprinted with permission from ref. [170]. Copyright 2016 Wiley-VCH Verlag GmbH & Co. KGaA, Weinheim.

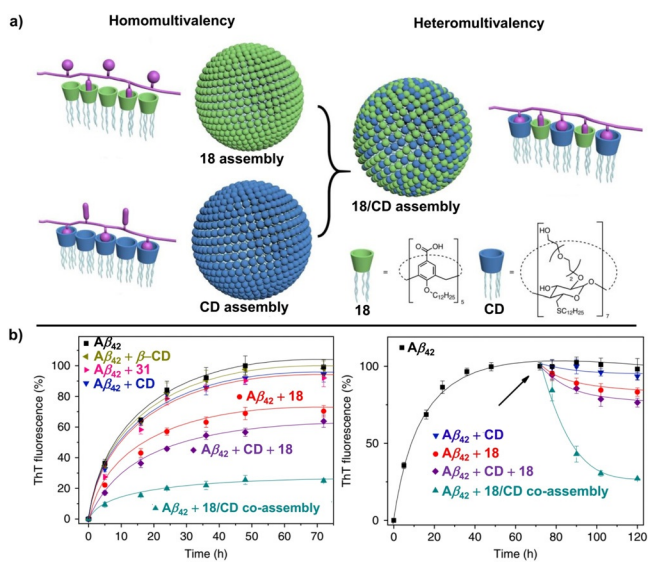


**Figure 23.** a) Heteromultivalent peptide recognition by the co-assembly of CD and **18** amphiphiles. b)  $\beta$ -sheet formation of  $\text{A}\beta_{42}$  monitored by ThT fluorescence in the absence and presence of indicated inhibitors. c) Disintegration of preformed  $\text{A}\beta_{42}$  fibrils by different disintegrators added to the solution of  $\text{A}\beta_{42}$  72 h after the initiation of aggregation. Reprinted with permission from ref. [53c]. Copyright 2019 Springer Nature.

guest for CD. The above platform provided not only multivalency but also heterotopicity (heteromultivalence), which resulted in a very strong affinity to  $\text{A}\beta_{42}$ . Hence, incubation of  $\text{A}\beta_{42}$  with an equimolar **18**/CD co-assembly resulted in a 75% reduction in ThT fluorescence intensity, i.e., in a 75% inhibition of  $\beta$ -sheet aggregation. The co-assembly could also disintegrate mature fibrils, which was more challenging and more important from the viewpoint of treatment. Furthermore, MTT assays showed that the **18**/CD co-assembly protected neuronal PC-12 cells from  $\text{A}\beta_{42}$ -induced cytotoxicity and itself exhibited little cytotoxicity at concentrations up to 40  $\mu\text{M}$ .

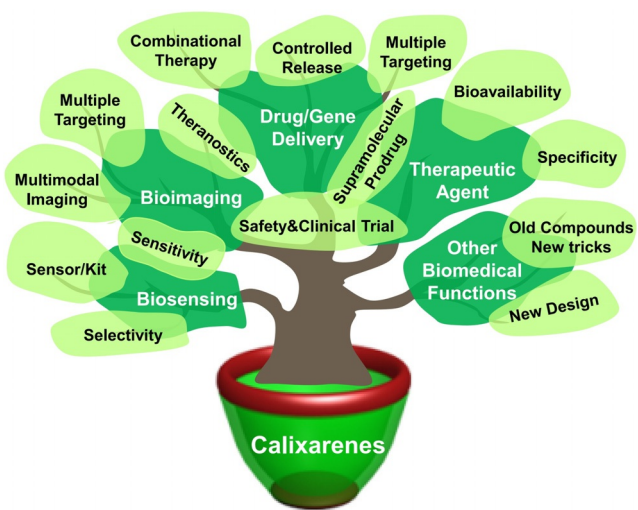
Mohanty et al. reported the inhibition and disintegration of insulin amyloid fibrils by **1** and **2**.<sup>[171]</sup> In the presence of 8 equiv of CAs, no fluorescence enhancement was observed during 400-min incubation, while fluorescence sharply increased after 90 min in the group without CAs. Furthermore, **1** and **2** also successfully disintegrated mature fibrils. The cell experiments demonstrated the potential utility of **1** and **2** as therapeutics for amyloidosis.

## 9. Summary and Outlook

In summary, CAs have been widely applied in biomedicine, e.g., for biosensing and bioimaging, contributing to *in vivo* and *in vitro* diagnosis.<sup>[172]</sup> Moreover, CAs have been used to construct drug and gene delivery systems, which contributed to targeted therapy. Additionally, the antibacterial, antiviral, anticancer, detoxification, and amyloid fibrillation inhibition activities of CAs promote the development of macrocyclic therapeutics. Such abundant biomedical applica-

tions benefit from the rich (supramolecular) chemistry of CAs and their broad chemical design space attributable to the ease of CA modification. The supramolecular chemistry of CAs paves the way to the exploration of biomedical functions. CAs have unique recognition properties, as their cavity can not only specifically recognize guests, but also quench the fluorescence and photoactivity of several dyes, which makes CAs suitable for turn-on fluorescence sensing, imaging, and activatable PDT. The CA skeleton can also be applied as a podand-like ligand for constructing novel recognition systems. CAs also possess excellent assembly properties. For example, because of their pre-organized framework, CA amphiphiles can form more stable and compact assemblies than the corresponding monomers. Therefore, amphiphilic CA-based drug/gene delivery systems often exhibit better performances than polymer-based ones. However, in contrast to polymers, CA amphiphiles have more defined molecular structures with precise size and molecular weights, which ensures batch-to-batch consistency and is an advantage for clinical translation and regulatory approval. Notably, the CA cavity size can be adjusted by changing the number of phenolic units and can be adapted to different functions. For example, the optimal cavity size of C5A allows it to selectively and strongly bind LPA, which cannot be achieved by either smaller or larger analogues.<sup>[80]</sup> CAs also exhibit the benefit of conformation controllability (and hence, control of physicochemical properties and biomedical functions). For example, guanidinium-modified C4A in cone conformation exhibits the highest DNA transfection efficiency, as it has a more suitable lipophilicity than C4As in 1,3-alternate and mobile conformations.<sup>[128a]</sup> These intrinsic features, including ease of modification, selective and strong binding to biological substrates, stable and compact assembly, tunable scaffold, and controllable conformation, collectively make CAs a privileged platform for diverse biomedical applications (Scheme 10).

Although these early works showed the biomedical potential of CA homologues for biosensing, bioimaging, drug/gene delivery, and therapeutics, examples of clinical CA use remain few at the time of this writing. The bench-to-bedside translation is highly demanded for the biomedical applications of CAs. Currently, one CA (**178**) is undergoing a phase-I clinical trial, which is a good trend. Nevertheless, CAs still face many practical challenges in biomedical applications from the viewpoints of both scientific research and clinical trials. For *in vitro* diagnosis, sensing systems should be further developed into sensors or even kits to make the biosensing application practical in clinical settings. For *in vivo* diagnosis and therapy, further studies of CA safety are required, e.g., those of long-term toxicity effects, metabolic pathways, and immunoreactions. With regard to optimization of diagnosis and therapy performance, some advanced modalities such as multimodal imaging, multiple targeting, and combination therapy can be employed and studied. Moreover, despite the large number of reported CA derivatives, their physicochemical properties and biomedical functions remain underexplored. Exploration of the new functions of existing CAs is imperative, requiring the collaborative efforts of multidisciplinary experts including those working in the



**Scheme 10.** Diverse biomedical applications of CAs and their perspectives.

fields of supramolecular chemistry, chemical biology, life sciences, pharmacy, and medicine. We think that numerous new tricks can still be accomplished with old molecules. In turn, one can summarize the inherent relationship between molecular structures and biomedical functions to guide the design of new CA derivatives. With continued research and development efforts, we believe that humanity will greatly benefit from CA-based biomedicine in the near future.

### Acknowledgements

This work was supported by NSFC (51873090, 21672112, and 31961143004) and the Fundamental Research Funds for the Central Universities.

### Conflict of interest

The authors declare no conflict of interest.

- [1] J. M. Lehn, *Chem. Soc. Rev.* **2017**, *46*, 2378–2379.
- [2] a) A. K. H. Hirsch, F. R. Fischer, F. Diederich, *Angew. Chem. Int. Ed.* **2007**, *46*, 338–352; *Angew. Chem.* **2007**, *119*, 342–357; b) R. Marchetti, S. Perez, A. Arda, A. Imberti, J. Jimenez-Barbero, A. Silipo, A. Molinaro, *ChemistryOpen* **2016**, *5*, 274–296.
- [3] W. W. Grabow, L. Jaeger, *Acc. Chem. Res.* **2014**, *47*, 1871–1880.
- [4] A. L. Horwitz, G. W. Farr, W. A. Fenton, *Chem. Rev.* **2006**, *106*, 1917–1930.
- [5] C. O. Mellet, J. M. García Fernandez, J. M. Benito, *Supramolecular Systems in Biomedical Fields*, Vol. 5, The Royal Society of Chemistry, London, **2013**, pp. 94–139.
- [6] T. Wang, X. Fan, C. Hou, J. Liu, *Curr. Opin. Struct. Biol.* **2018**, *51*, 19–27.
- [7] N. Sakai, S. Matile, *Langmuir* **2013**, *29*, 9031–9040.
- [8] K. Miyata, N. Nishiyama, K. Kataoka, *Chem. Soc. Rev.* **2012**, *41*, 2562–2574.
- [9] C. B. Rodell, J. E. Mealy, J. A. Burdick, *Bioconjugate Chem.* **2015**, *26*, 2279–2289.
- [10] H. Cui, B. Xu, *Chem. Soc. Rev.* **2017**, *46*, 6430–6432.
- [11] a) Y. Chen, Z. Huang, J.-F. Xu, Z. Sun, X. Zhang, *ACS Appl. Mater. Interfaces* **2016**, *8*, 22780–22784; b) J. Zhou, G. Yu, F. Huang, *Chem. Soc. Rev.* **2017**, *46*, 7021–7053.
- [12] a) X. Li, S. Lee, J. Yoon, *Chem. Soc. Rev.* **2018**, *47*, 1174–1188; b) G. Yu, X. Chen, *Theranostics* **2019**, *9*, 3041–3074.
- [13] A. G. Cheetham, R. W. Chakroun, W. Ma, H. Cui, *Chem. Soc. Rev.* **2017**, *46*, 6638–6663.
- [14] X. Ma, Y. Zhao, *Chem. Rev.* **2015**, *115*, 7794–7839.
- [15] a) Y. Chen, Y. Liu, *Chem. Soc. Rev.* **2010**, *39*, 495–505; b) G. Liu, Q. Yuan, G. Hollett, W. Zhao, Y. Kang, J. Wu, *Polym. Chem.* **2018**, *9*, 3436–3449; c) J. Zhang, P. X. Ma, *Nano Today* **2010**, *5*, 337–350.
- [16] T. Loftsson, D. Duchêne, *Int. J. Pharm.* **2007**, *329*, 1–11.
- [17] F. Cramer, *Einschlusverbindungen*, Springer, Berlin, **1954**, pp. 1–114.
- [18] a) N. Song, X.-Y. Lou, L. Ma, H. Gao, Y.-W. Yang, *Theranostics* **2019**, *9*, 3075–3093; b) R. Pinalli, E. Dalcanale, *Acc. Chem. Res.* **2013**, *46*, 399–411.
- [19] C. D. Gutsche, *Acc. Chem. Res.* **1983**, *16*, 161–170.
- [20] V. Böhmer, *Angew. Chem. Int. Ed. Engl.* **1995**, *34*, 713–745; *Angew. Chem.* **1995**, *107*, 785–818.
- [21] a) M. M. Naseer, M. Ahmed, S. Hameed, *Chem. Biol. Drug Des.* **2017**, *89*, 243–256; b) B. Mokhtari, K. Pourabdollah, *J. Inclusion Phenom. Macrocyclic Chem.* **2012**, *73*, 1–15; c) S. B. Nimse, T. Kim, *Chem. Soc. Rev.* **2013**, *42*, 366–386.
- [22] a) E. Da Silva, A. N. Lazar, A. W. Coleman, *J. Drug Delivery Sci. Technol.* **2004**, *14*, 3–20; b) S. Karakurt, T. F. Kellici, T. Mavromoustakos, A. G. Tzakos, M. Yilmaz, *Curr. Org. Chem.* **2016**, *20*, 1043–1057; c) M. Giuliani, I. Morbioli, F. Sansone, A. Casnati, *Chem. Commun.* **2015**, *51*, 14140–14159; d) D.-S. Guo, Y. Liu, *Acc. Chem. Res.* **2014**, *47*, 1925–1934; e) B. Mokhtari, K. Pourabdollah, *Drug Chem. Toxicol.* **2013**, *36*, 119–132; f) D. T. Schühle, J. A. Peters, J. Schatz, *Coord. Chem. Rev.* **2011**, *255*, 2727–2745; g) F. Perret, A. W. Coleman, *Chem. Commun.* **2011**, *47*, 7303–7319; h) B. Mokhtari, K. Pourabdollah, *J. Coord. Chem.* **2011**, *64*, 3189–3204; i) F. Sansone, L. Baldini, A. Casnati, R. Ungaro, *New J. Chem.* **2010**, *34*, 2715–2728; j) A. Dondoni, A. Marra, *Chem. Rev.* **2010**, *110*, 4949–4977; k) R. Kumar, A. Sharma, H. Singh, P. Suating, H. S. Kim, K. Sunwoo, I. Shim, B. C. Gibb, J. S. Kim, *Chem. Rev.* **2019**, *119*, 9657–9721.
- [23] A. Baeyer, *Ber. Dtsch. Chem. Ges.* **1872**, *5*, 1094–1100.
- [24] A. Zinke, E. Ziegler, *Ber. Dtsch. Chem. Ges.* **1944**, *77*, 264–272.
- [25] C. D. Gutsche, *Calixarenes Revisited*, Vol. 2–4, The Royal Society of Chemistry, London, **1998**, pp. 10–78.
- [26] K. Kogan, N. Itzhak, S. E. Biali, *Supramol. Chem.* **2010**, *22*, 704–709.
- [27] M. Bergamaschi, F. Bigi, M. Lanfranchi, R. Maggi, A. Pastorio, M. A. Pellinghelli, F. Peri, C. Porta, G. Sartori, *Tetrahedron* **1997**, *53*, 13037–13052.
- [28] H. Kumagai, M. Hasegawa, S. Miyanari, Y. Sugawa, Y. Sato, T. Hori, S. Ueda, H. Kamiyama, S. Miyano, *Tetrahedron Lett.* **1997**, *38*, 3971–3972.
- [29] a) X.-Y. Hu, S. Peng, D.-S. Guo, F. Ding, Y. Liu, *Supramol. Chem.* **2015**, *27*, 336–345; b) Y.-C. Pan, H.-W. Tian, S. Peng, X.-Y. Hu, D.-S. Guo, *Chin. Chem. Lett.* **2017**, *28*, 787–792.
- [30] H.-W. Tian, Y.-C. Pan, D.-S. Guo, *Supramol. Chem.* **2018**, *30*, 562–567.
- [31] a) F. Perret, A. N. Lazar, A. W. Coleman, *Chem. Commun.* **2006**, 2425–2438; b) D.-S. Guo, K. Wang, Y. Liu, *J. Inclusion Phenom. Macrocyclic Chem.* **2008**, *62*, 1–21; c) Y. Liu, Y.-H. Ma, Y. Chen, D.-S. Guo, Q. Li, *J. Org. Chem.* **2006**, *71*, 6468–6473.
- [32] Y.-Y. Wang, Y. Kong, Z. Zheng, W.-C. Geng, Z.-Y. Zhao, H. Sun, D.-S. Guo, *Beilstein J. Org. Chem.* **2019**, *15*, 1394–1406.

- [33] I. Leray, B. Valeur, *Eur. J. Inorg. Chem.* **2009**, 3525–3535.
- [34] a) H. M. Chawla, P. Goel, P. Munjal, *Tetrahedron Lett.* **2015**, 56, 682–685; b) A. Nehra, S. Bandaru, D. S. Yarramala, C. P. Rao, *Chem. Eur. J.* **2016**, 22, 8903–8914; c) A. Nehra, D. S. Yarramala, C. P. Rao, *Chem. Eur. J.* **2016**, 22, 8980–8989.
- [35] a) J.-P. Morel, N. Morel-Desrosiers, *Org. Biomol. Chem.* **2006**, 4, 462–465; b) M. Deska, B. Dondela, W. Sliwa, *ARKIVOC* **2015**, 4, 393–416.
- [36] Z. Xu, S. K. Kim, J. Yoon, *Chem. Soc. Rev.* **2010**, 39, 1457–1466.
- [37] a) Y. Liu, E.-C. Yang, Y. Chen, D.-S. Guo, F. Ding, *Eur. J. Org. Chem.* **2005**, 4581–4588; b) D.-S. Guo, L.-H. Wang, Y. Liu, *J. Org. Chem.* **2007**, 72, 7775–7778.
- [38] a) A. Ghoufi, J. P. Morel, N. Morel-Desrosiers, P. Malfreyt, *J. Phys. Chem. B* **2005**, 109, 23579–23587; b) S. Kunsagi-Máté, K. Szabó, I. Bitter, G. Nagy, L. Kollár, *J. Phys. Chem. A* **2005**, 109, 5237–5242; c) N. Kon, N. Iki, S. Miyano, *Org. Biomol. Chem.* **2003**, 1, 751–755.
- [39] a) F. Sansone, A. Casnati, *Chem. Soc. Rev.* **2013**, 42, 4623–4639; b) R. Ludwig, *Microchim. Acta* **2005**, 152, 1–19.
- [40] a) Y.-C. Liu, H. Sun, D.-S. Guo, *Curr. Org. Chem.* **2018**, 22, 2127–2149; b) H.-W. Tian, Y.-C. Liu, D.-S. Guo, *Mater. Chem. Front.* **2020**, 4, 46–98.
- [41] K. Jie, Y. Zhou, Y. Yao, F. Huang, *Chem. Soc. Rev.* **2015**, 44, 3568–3587.
- [42] G. Yu, K. Jie, F. Huang, *Chem. Rev.* **2015**, 115, 7240–7303.
- [43] X. Zhang, C. Wang, *Chem. Soc. Rev.* **2011**, 40, 94–101.
- [44] D.-S. Guo, B.-P. Jiang, X. Wang, Y. Liu, *Org. Biomol. Chem.* **2012**, 10, 720–723.
- [45] Y. Tauran, A. W. Coleman, F. Perret, B. Kim, *Curr. Org. Chem.* **2015**, 19, 2250–2270.
- [46] E. Da Silva, P. Shahgaldian, A. W. Coleman, *Int. J. Pharm.* **2004**, 273, 57–62.
- [47] M.-H. Paclet, C. F. Rousseau, C. Yannick, F. Morel, A. W. Coleman, *J. Inclusion Phenom. Macrocyclic Chem.* **2006**, 55, 353–357.
- [48] A. W. Coleman, S. Jebors, S. Cecillon, P. Perret, D. Garin, D. Marti-Battle, M. Moulin, *New J. Chem.* **2008**, 32, 780–782.
- [49] N. J. Wheate, G. M. Abbott, R. J. Tate, C. J. Clements, R. Edrada-Ebel, B. F. Johnston, *J. Inorg. Biochem.* **2009**, 103, 448–454.
- [50] A. D. Martin, E. Houlihan, N. Morellini, P. K. Eggers, E. James, K. A. Stubbs, A. R. Harvey, M. Fitzgerald, C. L. Raston, S. A. Dunlop, *ChemPlusChem* **2012**, 77, 308–313.
- [51] W.-C. Geng, S. Jia, Z. Zheng, Z. Li, D. Ding, D.-S. Guo, *Angew. Chem. Int. Ed.* **2019**, 58, 2377–2381; *Angew. Chem.* **2019**, 131, 2399–2403.
- [52] E. V. Ukhatskaya, S. V. Kurkov, M. A. Hjalmarsdottir, V. A. Karginov, S. E. Matthews, R. V. Rodik, V. I. Kalchenko, T. Loftsson, *Int. J. Pharm.* **2013**, 458, 25–30.
- [53] a) J. Gao, J. Li, W.-C. Geng, F.-Y. Chen, X. Duan, Z. Zheng, D. Ding, D.-S. Guo, *J. Am. Chem. Soc.* **2018**, 140, 4945–4953; b) C. Tu, L. Zhu, P. Li, Y. Chen, Y. Su, D. Yan, X. Zhu, G. Zhou, *Chem. Commun.* **2011**, 47, 6063–6065; c) Z. Xu, S. Jia, W. Wang, Z. Yuan, B. Jan Ravoo, D.-S. Guo, *Nat. Chem.* **2019**, 11, 86–93.
- [54] S. M. Sebti, A. D. Hamilton, *Oncogene* **2000**, 19, 6566–6573.
- [55] S. Viola, S. Merlo, G. M. L. Consoli, F. Drago, C. Geraci, M. A. Sortino, *Pharmacol.* **2010**, 86, 182–188.
- [56] A. Galukhin, I. Imatdinov, Y. Osin, *RSC Adv.* **2016**, 6, 32722–32726.
- [57] a) G. Arena, A. Casnati, A. Contino, A. Magri, F. Sansone, D. Sciutto, R. Ungaro, *Org. Biomol. Chem.* **2006**, 4, 243–249; b) L. Mutihac, J. H. Lee, J. S. Kim, J. Vicens, *Chem. Soc. Rev.* **2011**, 40, 2777–2796; c) T. Gruber, *ChemBioChem* **2018**, 19, 2324–2359; d) A. W. Coleman, F. Perret, A. Moussa, M. Dupin, Y. Gu, H. Perron, in *Creative Chemical Sensor Systems*, Vol. 277 (Ed.: T. Schrader), Springer-Verlag, Berlin Heidelberg, **2007**, pp. 31–88; e) R. Zadmard, N. S. Alavijeh, *RSC Adv.* **2014**, 4, 41529–41542; f) K. Kurzatkowska, S. Sayin, M. Yilmaz, H. Radecka, J. Radecki, *Sens. Actuators B* **2015**, 218, 111–121.
- [58] L. You, D. Zha, E. V. Anslyn, *Chem. Rev.* **2015**, 115, 7840–7892.
- [59] R. N. Dsouza, A. Hennig, W. M. Nau, *Chem. Eur. J.* **2012**, 18, 3444–3459.
- [60] a) F. Ahmed, S. Perveen, K. Shah, M. R. Shah, S. Ahmed, *Ecotoxicol. Environ. Saf.* **2018**, 147, 49–54; b) E. Khaled, M. M. Khalil, G. M. A. el Aziz, *Sens. Actuators B* **2017**, 244, 876–884; c) Y. Zhou, H. Xu, H. Yu, L. Chun, Q. Lu, L. Wang, *Spectrochim. Acta Part A* **2008**, 70, 411–415; d) X. Wang, C. Luo, Z. Lv, F. Lu, *J. Lumin.* **2011**, 131, 1986–1990; e) J. Gao, Z. Zheng, L. Shi, S.-Q. Wu, H. Sun, D.-S. Guo, *Beilstein J. Org. Chem.* **2018**, 14, 1840–1845; f) L. Yang, X. Xie, L. Cai, X. Ran, Y. Li, T. Yin, H. Zhao, C.-P. Li, *Biosens. Bioelectron.* **2016**, 82, 146–154; g) L. Ma, X. Zhu, *Spectrochim. Acta Part A* **2012**, 95, 246–251; h) M. T. Ragab, M. K. Abd El-Rahman, N. K. Ramadan, N. A. El-Ragehy, B. A. El-Zeany, *Talanta* **2015**, 138, 28–35; i) M. A. El-Sayed, *Sens. Actuators B* **2014**, 190, 101–110; j) E. V. Ukhatskaya, S. V. Kurkov, S. E. Matthews, T. Loftsson, *J. Pharm. Sci.* **2013**, 102, 3485–3512; k) H. Zhao, L. Yang, Y. Li, X. Ran, H. Ye, G. Zhao, Y. Zhang, F. Liu, C.-P. Li, *Biosens. Bioelectron.* **2017**, 89, 361–369; l) C. Meenakshi, P. Jayabal, V. Ramakrishnan, *Spectrochim. Acta Part A* **2015**, 151, 707–711; m) C. Meenakshi, P. Jayabal, V. Ramakrishnan, *Spectrochim. Acta Part A* **2014**, 122, 447–450; n) J. V. de Assis, M. G. Teixeira, C. G. P. Soares, J. F. Lopes, G. S. L. Carvalho, M. C. S. Lourenco, M. V. de Almeida, W. B. de Almeida, S. A. Fernandes, *Eur. J. Pharm. Sci.* **2012**, 47, 539–548; o) J. G. Panchal, R. V. Patel, S. K. Menon, *J. Inclusion Phenom. Macrocyclic Chem.* **2010**, 67, 201–208; p) H. Li, J.-P. Song, J.-B. Chao, S.-M. Shuang, C. Dong, *Spectrochim. Acta Part A* **2012**, 97, 155–160; q) L. M. Arantes, C. Scarelli, A. J. Marsaioli, E. de Paula, S. A. Fernandes, *Magn. Reson. Chem.* **2009**, 47, 757–763; r) S. A. Fernandes, L. F. Cabeca, A. J. Marsaioli, E. de Paula, *J. Inclusion Phenom. Macrocyclic Chem.* **2007**, 57, 395–401; s) A. M. El-Kosasy, M. Nebsen, M. K. Abd El-Rahman, M. Y. Salem, M. G. El-Bardicy, *Talanta* **2011**, 85, 913–918; t) H. AlRabiah, *Int. J. Electrochem. Sci.* **2016**, 11, 6761–6774; u) N. F. Abo-Talib, M. H. Tammam, A. K. Attia, *RSC Adv.* **2015**, 5, 95592–95597; v) M. A. Hussain, M. U. Ashraf, G. Muhammad, M. N. Tahir, S. N. A. Bukhari, *Curr. Pharm. Des.* **2017**, 23, 2377–2388.
- [61] a) H. M. Chawla, P. Goel, R. Shukla, D. S. C. Black, N. Kumar, *J. Inclusion Phenom. Macrocyclic Chem.* **2014**, 80, 201–207; b) R. Joseph, B. Ramanujam, A. Acharya, C. P. Rao, *Tetrahedron Lett.* **2009**, 50, 2735–2739; c) H. J. Kim, S. H. Kim, J. H. Kim, L. N. Anh, J. H. Lee, C.-H. Lee, J. S. Kim, *Tetrahedron Lett.* **2009**, 50, 2782–2786; d) R. Gunupuru, D. Maity, G. R. Bhadu, A. Chakraborty, D. N. Srivastava, P. Paul, *J. Chem. Sci.* **2014**, 126, 627–635; e) V. V. S. Mummidivarapu, V. K. Hinge, K. Tabbasum, R. G. Gonnade, C. P. Rao, *J. Org. Chem.* **2013**, 78, 3570–3576; f) V. V. S. Mummidivarapu, D. S. Yarramala, K. K. Kondaveeti, C. P. Rao, *J. Org. Chem.* **2014**, 79, 10477–10486; g) M. Esmaielzade Rostami, B. Gorji, R. Zadmard, *J. Heterocycl. Chem.* **2018**, 55, 2532–2537; h) P. Fan, L. Wan, Y. Shang, J. Wang, Y. Liu, X. Sun, C. Chen, *Bioorg. Chem.* **2015**, 58, 88–95; i) B. Lotfi, A. Tarlani, P. Akbari-Moghaddam, M. Mirza-Aghayan, A. A. Peyghan, J. Muzart, R. Zadmard, *Biosens. Bioelectron.* **2017**, 90, 290–297; j) M.-C. Oh, K.-J. Kim, J.-H. Lee, H.-X. Chen, K.-N. Koh, *Appl. Phys. Lett.* **2006**, 89, 251104; k) G.-S. Lai, H.-L. Zhang, C.-M. Jin, *Electroanalysis* **2007**, 19, 496–501; l) G. A. Evtugyn, R. V. Shamagsumova, R. R. Sitdikov, I. I. Stoikov, I. S. Antipin, M. V. Ageeva, T. Hianik, *Electroanalysis* **2011**, 23, 2281–2289; m) H.-L. Zhang, Y. Liu, G.-S. Lai, A.-M. Yu, Y.-M. Huang, C.-M. Jin, *Analyst* **2009**, 134,

- 2141–2146; n) D. Maity, A. Kumar, R. Gunupuru, P. Paul, *Colloids Surf. A* **2014**, *455*, 122–128; o) L. Yang, L. Luo, G. Zhang, F. Miao, X. Zhang, D. Tian, H. Li, *ChemPlusChem* **2013**, *78*, 1517–1522; p) M. Song, Z. Sun, C. Han, D. Tian, H. Li, L. Jiang, *Chem. Eur. J.* **2014**, *20*, 7987–7993.
- [62] A. Depauw, E. Dossi, N. Kumar, C. Fiorini-Debuisschert, G. Huberfeld, M.-H. Ha-Thi, N. Rouach, I. Leray, *Chem. Eur. J.* **2016**, *22*, 14902–14911.
- [63] R. K. Pathak, A. G. Dikundwar, T. N. G. Row, C. P. Rao, *Chem. Commun.* **2010**, *46*, 4345–4347.
- [64] V. V. Sreenivasu Mummidivarapu, V. K. Hinge, K. Samanta, D. S. Yaramala, C. P. Rao, *Chem. Eur. J.* **2014**, *20*, 14378–14386.
- [65] B. Khan, M. R. Shah, D. Ahmed, M. Rabnawaz, I. Anis, S. Afridi, T. Makhmoor, M. N. Tahir, *J. Hazard. Mater.* **2016**, *309*, 97–106.
- [66] P. G. Sutariya, A. Pandya, A. Lodha, S. K. Menon, *Analyst* **2014**, *139*, 4794–4798.
- [67] a) S. Tanwar, J.-a. A. Ho, E. Magi, *Talanta* **2013**, *117*, 352–358; b) G. Zheng, M. Chen, X. Liu, J. Zhou, J. Xie, G. Diao, *Electrochim. Acta* **2014**, *136*, 301–309; c) P. M. Mareeswaran, M. Prakash, V. Subramanian, S. Rajagopal, *J. Phys. Org. Chem.* **2012**, *25*, 1217–1227; d) E. K. Wujcik, N. J. Blasdel, D. Trowbridge, C. N. Monty, *IEEE Sens. J.* **2013**, *13*, 3430–3436; e) M. Šnejdárková, A. Poturnayová, P. Rybář, P. Lhoták, M. Himpl, K. Flídrová, T. Hianik, *Bioelectrochemistry* **2010**, *80*, 55–61; f) B. Wu, F. Zou, X. Wang, K. Koh, K. Wang, H. Chen, *Anal. Methods* **2017**, *9*, 2153–2158; g) M. A. Mohsin, B. D. Liu, X. L. Zhang, W. J. Yang, L. S. Liu, X. Jiang, *RSC Adv.* **2017**, *7*, 3012–3020; h) Y. Xu, Q. Hao, D. Mandler, *Anal. Chim. Acta* **2018**, *1042*, 29–36.
- [68] a) Y. Chen, J. Zhang, Y. Gao, J. Lee, H. Chen, Y. Yin, *Biosens. Bioelectron.* **2015**, *72*, 306–312; b) A. Pandya, P. G. Sutariya, S. K. Menon, *Analyst* **2013**, *138*, 2483–2490; c) P. G. Sutariya, A. Pandya, A. Lodha, S. K. Menon, *Talanta* **2016**, *147*, 590–597.
- [69] T. Jin, F. Fujii, H. Sakata, M. Tamura, M. Kinjo, *Chem. Commun.* **2005**, 4300–4302.
- [70] R. Zadmard, M. Arendt, T. Schrader, *J. Am. Chem. Soc.* **2004**, *126*, 7752–7753.
- [71] R. Zadmard, T. Schrader, *J. Am. Chem. Soc.* **2005**, *127*, 904–915.
- [72] S. Kolusheva, R. Zadmard, T. Schrader, R. Jelinek, *J. Am. Chem. Soc.* **2006**, *128*, 13592–13598.
- [73] B. T. Nguyen, E. V. Anslyn, *Coord. Chem. Rev.* **2006**, *250*, 3118–3127.
- [74] M. A. Beatty, J. Borges-Gonzalez, N. J. Sinclair, A. T. Pye, F. Hof, *J. Am. Chem. Soc.* **2018**, *140*, 3500–3504.
- [75] H. Bakirci, W. M. Nau, *Adv. Funct. Mater.* **2006**, *16*, 237–242.
- [76] N. Korbakov, P. Timmerman, N. Lidich, B. Urbach, A. Sa'ar, S. Yitzchaik, *Langmuir* **2008**, *24*, 2580–2587.
- [77] T. Jin, F. Fujii, Y. Ooi, *Sensors* **2008**, *8*, 6777–6790.
- [78] T. Jin, *Sensors* **2010**, *10*, 2438–2449.
- [79] a) T. Jin, *J. Inclusion Phenom. Macrocyclic Chem.* **2003**, *45*, 195–201; b) Q. Lu, J. Gu, H. Yu, C. Liu, L. Wang, Y. Zhou, *Spectrochim. Acta Part A* **2007**, *68*, 15–20; c) X. Mao, D. Tian, H. Li, *Chem. Commun.* **2012**, *48*, 4851–4853.
- [80] G. B. Mills, W. H. Moolenaar, *Nat. Rev. Cancer* **2003**, *3*, 582–591.
- [81] Z. Zheng, W.-C. Geng, J. Gao, Y.-Y. Wang, H. Sun, D.-S. Guo, *Chem. Sci.* **2018**, *9*, 2087–2091.
- [82] M. A. Beatty, A. J. Selinger, Y. Li, F. Hof, *J. Am. Chem. Soc.* **2019**, *141*, 16763–16771.
- [83] a) K. D. Daze, F. Hof, *Acc. Chem. Res.* **2013**, *46*, 937–945; b) K. D. Daze, M. C. F. Ma, F. Pineux, F. Hof, *Org. Lett.* **2012**, *14*, 1512–1515; c) K. D. Daze, C. E. Jones, B. J. Lilgert, C. S. Beshara, F. Hof, *Can. J. Chem.* **2013**, *91*, 1072–1076; d) C. S. Beshara, C. E. Jones, K. D. Daze, B. J. Lilgert, F. Hof, *ChemBioChem* **2010**, *11*, 63–66; e) K. D. Daze, T. Pinter, C. S. Beshara, A. Ibraheem, S. A. Minaker, M. C. F. Ma, R. J. M. Courtemanche, R. E. Campbell, F. Hof, *Chem. Sci.* **2012**, *3*, 2695; f) S. Tabet, S. F. Douglas, K. D. Daze, G. A. E. Garnett, K. J. H. Allen, E. M. M. Abrioux, T. T. H. Quon, J. E. Wulff, F. Hof, *Bioorg. Med. Chem.* **2013**, *21*, 7004–7010; g) G. A. E. Garnett, M. J. Starke, A. Shaurya, J. Li, F. Hof, *Anal. Chem.* **2016**, *88*, 3697–3703.
- [84] S. A. Minaker, K. D. Daze, M. C. Ma, F. Hof, *J. Am. Chem. Soc.* **2012**, *134*, 11674–11680.
- [85] Z. Zheng, W.-C. Geng, J. Gao, Y.-J. Mu, D.-S. Guo, *Org. Chem. Front.* **2018**, *5*, 2685–2691.
- [86] a) A. Hennig, H. Bakirci, W. M. Nau, *Nat. Methods* **2007**, *4*, 629–632; b) M. Florea, W. M. Nau, *Org. Biomol. Chem.* **2010**, *8*, 1033–1039.
- [87] W. M. Nau, G. Ghale, A. Hennig, H. Bakirci, D. M. Bailey, *J. Am. Chem. Soc.* **2009**, *131*, 11558–11570.
- [88] a) D.-S. Guo, V. D. Uzunova, X. Su, Y. Liu, W. M. Nau, *Chem. Sci.* **2011**, *2*, 1722–1734; b) M. Florea, S. Kudithipudi, A. Rei, M. J. González-Álvarez, A. Jeltsch, W. M. Nau, *Chem. Eur. J.* **2012**, *18*, 3521–3528.
- [89] D.-S. Guo, J. Yang, Y. Liu, *Chem. Eur. J.* **2013**, *19*, 8755–8759.
- [90] S. Peng, A. Barba-Bon, Y.-C. Pan, W. M. Nau, D.-S. Guo, A. Hennig, *Angew. Chem. Int. Ed.* **2017**, *56*, 15742–15745; *Angew. Chem.* **2017**, *129*, 15948–15951.
- [91] a) G. Ghale, W. M. Nau, *Acc. Chem. Res.* **2014**, *47*, 2150–2159; b) A. Barba-Bon, Y.-C. Pan, F. Biedermann, D.-S. Guo, W. M. Nau, A. Hennig, *J. Am. Chem. Soc.* **2019**, *141*, 20137–20145.
- [92] G. Ghale, A. G. Lanctot, H. T. Kreissl, M. H. Jacob, H. Weingart, M. Winterhalter, W. M. Nau, *Angew. Chem. Int. Ed.* **2014**, *53*, 2762–2765; *Angew. Chem.* **2014**, *126*, 2801–2805.
- [93] A. Norouzy, Z. Azizi, W. M. Nau, *Angew. Chem. Int. Ed.* **2015**, *54*, 792–795; *Angew. Chem.* **2015**, *127*, 804–808.
- [94] B. Pelaz, C. Alexiou, R. A. Alvarez-Puebla, F. Alves, A. M. Andrews, S. Ashraf, L. P. Balogh, L. Ballerini, A. Bestetti, C. Brendel, S. Bosi, M. Carril, W. C. Chan, C. Chen, X. Chen, X. Chen, Z. Cheng, D. Cui, J. Du, C. Dullin, A. Escudero, N. Feliu, M. Gao, M. George, Y. Gogotsi, A. Grunweller, Z. Gu, N. J. Halas, N. Hampp, R. K. Hartmann, M. C. Hersam, P. Hunziker, J. Jian, X. Jiang, P. Jungebluth, P. Kadzhiresan, K. Kataoka, A. Khademhosseini, J. Kopecek, N. A. Kotov, H. F. Krug, D. S. Lee, C. M. Lehr, K. W. Leong, X. J. Liang, M. Ling Lim, L. M. Liz-Marzan, X. Ma, P. Macchiarini, H. Meng, H. Mohwald, P. Mulvaney, A. E. Nel, S. Nie, P. Nordlander, T. Okano, J. Oliveira, T. H. Park, R. M. Penner, M. Prato, V. Puntes, V. M. Rotello, A. Samarakoon, R. E. Schaak, Y. Shen, S. Sjoqvist, A. G. Skirtach, M. G. Soliman, M. M. Stevens, H. W. Sung, B. Z. Tang, R. Tietze, B. N. Udagama, J. S. VanEpps, T. Weil, P. S. Weiss, I. Willner, Y. Wu, L. Yang, Z. Yue, Q. Zhang, Q. Zhang, X. E. Zhang, Y. Zhao, X. Zhou, W. J. Parak, *ACS Nano* **2017**, *11*, 2313–2381.
- [95] a) R. Pinalli, A. Pedrini, E. Dalcanale, *Chem. Soc. Rev.* **2018**, *47*, 7006–7026; b) R. Lalor, H. Baillie-Johnson, C. Redshaw, S. E. Matthews, A. Mueller, *J. Am. Chem. Soc.* **2008**, *130*, 2892–2893; c) A. Mueller, R. Lalor, C. M. Cardaba, S. E. Matthews, *Cytometry Part A* **2011**, *79*, 126–136; d) S. Erdemir, O. Kocayigit, S. Karakurt, *Sens. Actuators B* **2015**, *220*, 381–388; e) M. Oğuz, A. A. Bhatti, S. Karakurt, M. Aktas, M. Yilmaz, *Spectrochim. Acta Part A* **2017**, *171*, 340–345; f) H. Kaur, P. Raj, H. Sharma, M. Verma, N. Singh, N. Kaur, *Anal. Chim. Acta* **2018**, *1009*, 1–11.
- [96] X.-M. Chen, Y. Chen, Q. Yu, B.-H. Gu, Y. Liu, *Angew. Chem. Int. Ed.* **2018**, *57*, 12519–12523; *Angew. Chem.* **2018**, *130*, 12699–12703.
- [97] I. Shulov, R. V. Rodik, Y. Arntz, A. Reisch, V. I. Kalchenko, A. S. Klymchenko, *Angew. Chem. Int. Ed.* **2016**, *55*, 15884–15888; *Angew. Chem.* **2016**, *128*, 16116–16120.

- [98] S. Aime, A. Barge, M. Botta, A. Casnati, M. Fragai, C. Luchinat, R. Ungaro, *Angew. Chem. Int. Ed.* **2001**, *40*, 4737–4739; *Angew. Chem.* **2001**, *113*, 4873–4875.
- [99] a) D. T. Schühle, M. Polášek, I. Lukeš, T. Chauvin, E. Tóth, J. Schatz, U. Hanefeld, M. C. Stuart, J. A. Peters, *Dalton Trans.* **2010**, *39*, 185–191; b) D. T. Schühle, J. Schatz, S. Laurent, L. Vander Elst, R. N. Muller, M. C. Stuart, J. A. Peters, *Chem. Eur. J.* **2009**, *15*, 3290–3296.
- [100] Z. Zheng, W. C. Geng, Z. Xu, D. S. Guo, *Isr. J. Chem.* **2019**, *59*, 913–927.
- [101] A. Kakkar, G. Traverso, O. C. Farokhzad, R. Weissleder, R. Langer, *Nat. Rev. Chem.* **2017**, *1*, 1–17.
- [102] a) J. Chao, Y. Zhang, X. Fan, H. Wang, Y. Li, *Spectrochim. Acta Part A* **2013**, *116*, 295–300; b) W. Yang, M. M. de Villiers, *Eur. J. Pharm. Biopharm.* **2004**, *58*, 629–636; c) W. Yang, M. M. de Villiers, *J. Pharm. Pharmacol.* **2004**, *56*, 703–708; d) L. M. Arantes, E. V. V. Varejão, K. J. Pelizzaro-Rocha, C. M. S. Cereda, E. de Paula, M. P. Lourenço, H. A. Duarte, S. A. Fernandes, *Chem. Biol. Drug Des.* **2014**, *83*, 550–559; e) K. Khan, S. L. Badshah, N. Ahmad, H. U. Rashid, Y. Mabkhot, *Molecules* **2017**, *22*, 783–792; f) H. Huang, D.-M. Li, W. Wang, Y.-C. Chen, K. Khan, S. Song, Y.-S. Zheng, *Org. Biomol. Chem.* **2012**, *10*, 729–735; g) J. Mo, L. Wang, X. Huang, B. Lu, C. Zou, L. Wei, J. Chu, P. K. Eggers, S. Chen, C. L. Raston, J. Wu, L. Y. Lim, W. Zhao, *Nanoscale* **2017**, *9*, 13142–13152; h) D. Shetty, T. Skorjanc, M. A. Olson, A. Trabolsi, *Chem. Commun.* **2019**, *55*, 8876–8879; i) C. Mehra, R. Gala, A. Kakatkar, V. Kumar, R. Khurana, S. Chatterjee, N. N. Kumar, N. Barooah, A. C. Bhasikuttan, J. Mohanty, *Chem. Commun.* **2019**, *55*, 14275–14278.
- [103] S. K. Menon, B. R. Mistry, K. V. Joshi, N. R. Modi, D. Shashtri, *J. Inclusion Phenom. Macrocyclic Chem.* **2012**, *73*, 295–303.
- [104] J. Mo, P. K. Eggers, X. Chen, M. R. H. Ahamed, T. Becker, L. Y. Lim, C. L. Raston, *Sci. Rep.* **2015**, *5*, 10414.
- [105] J. Gao, H. Yu, F.-Y. Chen, X.-Y. Hu, Y. Wang, D.-S. Guo, *Chem. Commun.* **2019**, *55*, 14387–14390.
- [106] a) E. V. Ukhatskaya, S. V. Kurkov, S. E. Matthews, A. El Fagui, C. Amiel, F. Dalmas, T. Loftsson, *Int. J. Pharm.* **2010**, *402*, 10–19; b) I. Jelezova, E. Drakalska, D. Momekova, N. Shalimova, G. Momekov, S. Konstantinov, S. Rangelov, S. Pispas, *Eur. J. Pharm. Sci.* **2015**, *78*, 67–78; c) L. Gallego-Yerga, I. Posadas, C. de la Torre, J. Ruiz-Almansa, F. Sansone, C. Ortiz Mellet, A. Casnati, J. M. Garcia Fernandez, V. Cena, *Front. Pharmacol.* **2017**, *8*, 249–261; d) C. Weeden, K. J. Hartlieb, L. Y. Lim, *J. Pharm. Pharmacol.* **2012**, *64*, 1403–1411; e) S. Fujii, K. Nishina, S. Yamada, S. Mochizuki, N. Ohta, A. Takahara, K. Sakurai, *Soft Matter* **2014**, *10*, 8216–8223; f) L. Barbera, G. Gattuso, F. H. Kohnke, A. Notti, S. Pappalardo, M. F. Parisi, I. Pisagatti, S. Patanè, N. Micali, V. Villari, *Org. Biomol. Chem.* **2015**, *13*, 6468–6473; g) I. Di Bari, R. Picciotto, G. Granata, A. R. Blanco, G. M. L. Consoli, S. Sortino, *Org. Biomol. Chem.* **2016**, *14*, 8047–8052; h) E. James, P. K. Eggers, A. R. Harvey, S. A. Dunlop, M. Fitzgerald, K. A. Stubbs, C. L. Raston, *Org. Biomol. Chem.* **2013**, *11*, 6108–6112; i) M.-X. Chen, T. Li, S. Peng, D. Tao, *New J. Chem.* **2016**, *40*, 9923–9929; j) L. Gallego-Yerga, M. Lomazzi, F. Sansone, C. Ortiz Mellet, A. Casnati, J. M. Garcia Fernandez, *Chem. Commun.* **2014**, *50*, 7440–7443; k) E. Drakalska, D. Momekova, Y. Manolova, D. Budurova, G. Momekov, M. Genova, L. Antonov, N. Lambov, S. Rangelov, *Int. J. Pharm.* **2014**, *472*, 165–174; l) J. Mo, P. K. Eggers, Z.-X. Yuan, C. L. Raston, L. Y. Lim, *Sci. Rep.* **2016**, *6*, 23489.
- [107] W. Chen, L. Li, X. Zhang, Y. Liang, Z. Pu, L. Wang, J. Mo, *Drug Delivery* **2017**, *24*, 1470–1481.
- [108] G. Granata, I. Paterniti, C. Geraci, F. Cunsolo, E. Esposito, M. Cordaro, A. R. Blanco, S. Cuzzocrea, G. M. L. Consoli, *Mol. Pharm.* **2017**, *14*, 1610–1622.
- [109] I. Pisagatti, L. Barbera, G. Gattuso, S. Patanè, M. F. Parisi, A. Notti, *Supramol. Chem.* **2018**, *30*, 658–663.
- [110] D.-S. Guo, K. Wang, Y.-X. Wang, Y. Liu, *J. Am. Chem. Soc.* **2012**, *134*, 10244–10250.
- [111] K. Wang, D.-S. Guo, M.-Y. Zhao, Y. Liu, *Chem. Eur. J.* **2016**, *22*, 1475–1483.
- [112] Z. Qin, D.-S. Guo, X.-N. Gao, Y. Liu, *Soft matter* **2014**, *10*, 2253–2263.
- [113] Y.-X. Wang, D.-S. Guo, Y.-C. Duan, Y.-J. Wang, Y. Liu, *Sci. Rep.* **2015**, *5*, 9019.
- [114] M. V. Ramakrishnam Raju, H.-C. Lin, *J. Mater. Chem. A* **2015**, *3*, 6414–6422.
- [115] Y.-L. Sun, Y. Zhou, Q.-L. Li, Y.-W. Yang, *Chem. Commun.* **2013**, *49*, 9033–9035.
- [116] Y. Zhou, L.-L. Tan, Q.-L. Li, X.-L. Qiu, A.-D. Qi, Y. Tao, Y.-W. Yang, *Chem. Eur. J.* **2014**, *20*, 2998–3004.
- [117] T. Zhou, N. Song, S.-H. Xu, B. Dong, Y.-W. Yang, *ChemPhysChem* **2016**, *17*, 1840–1845.
- [118] L. Jin, X. Zeng, M. Liu, Y. Deng, N. He, *Theranostics* **2014**, *4*, 240–255.
- [119] M. Nishikawa, L. Huang, *Hum. Gene Ther.* **2001**, *12*, 861–870.
- [120] S. Paul, E. Regulier, R. Rooke, F. Stoeckel, M. Geist, H. Homann, J.-M. Balloul, D. Villeval, Y. Poitevin, M.-P. Kiény, R. B. Acres, *Cancer Gene Ther.* **2002**, *9*, 470–477.
- [121] a) Q. Lin, J. Chen, Z. Zhang, G. Zheng, *Nanomedicine* **2014**, *9*, 105–120; b) B. Zheng, F. Wang, S. Dong, F. Huang, *Chem. Soc. Rev.* **2012**, *41*, 1621–1636; c) J. Yang, Q. Zhang, H. Chang, Y. Cheng, *Chem. Rev.* **2015**, *115*, 5274–5300; d) W.-C. Geng, Q. Huang, Z. Xu, R. Wang, D.-S. Guo, *Theranostics* **2019**, *9*, 3094–3106.
- [122] X. Zhou, P. Pathak, J. Jayawickramarajah, *Chem. Commun.* **2018**, *54*, 11668–11680.
- [123] a) T. Schrader, C. Blecking, W. Hu, R. Zadmard, A. Dasgupta, *Synthesis* **2011**, *2011*, 1193–1204; b) B. Khairutdinov, E. Ermakova, A. Sitnitsky, I. Stoikov, Y. Zuev, *J. Mol. Struct.* **2014**, *1074*, 126–133; c) J. Chao, H. F. Wang, Y. Zhang, F. Huo, C. Yin, *Spectrochim. Acta Part A* **2013**, *103*, 73–78; d) R. Zadmard, S. Taghvaei-Ganjali, B. Gorji, T. Schrader, *Chem. Asian J.* **2009**, *4*, 1458–1464; e) A. Galukhin, A. Erokhin, I. Imatinidin, Y. Osin, *RSC Adv.* **2015**, *5*, 33351–33355; f) V. Rullaud, N. Moridi, P. Shahgaldian, *Langmuir* **2014**, *30*, 8675–8679; g) W. Hu, C. Blecking, M. Kralj, L. Suman, I. Piantanida, T. Schrader, *Chem. Eur. J.* **2012**, *18*, 3589–3597.
- [124] N. S. Alavijeh, R. Zadmard, S. Balalaie, M. S. Alavijeh, N. Soltani, *Org. Lett.* **2016**, *18*, 4766–4769.
- [125] W. Janrungratsakul, T. Vilaivan, C. Vilaivan, S. Watchasit, C. Suksai, W. Ngeontae, W. Aeungmaitrepirom, T. Tuntulani, *Talanta* **2013**, *105*, 1–7.
- [126] F. J. Ostos, J. A. Lebron, M. L. Moyá, M. Deasy, P. López-Cornejo, *Colloids Surf. B* **2015**, *127*, 65–72.
- [127] a) C. Ortiz Mellet, J. M. Benito, J. M. García Fernández, *Chem. Eur. J.* **2010**, *16*, 6728–6742; b) A. Zheng, Y. Xue, D. Wei, Y. Guan, H. Xiao, *Mater. Sci. Eng.* **2013**, *33*, 519–526; c) L. Nault, A. Cumbo, R. F. Pretot, M. A. Sciotti, P. Shahgaldian, *Chem. Commun.* **2010**, *46*, 5581–5583; d) R. Lalor, J. L. DiGesso, A. Mueller, S. E. Matthews, *Chem. Commun.* **2007**, 4907–4909; e) T. Takeuchi, V. Bagnacani, F. Sansone, S. Matile, *ChemBioChem* **2009**, *10*, 2793–2799; f) L. Gallego-Yerga, M. Lomazzi, V. Franceschi, F. Sansone, C. Ortiz Mellet, G. Donofrio, A. Casnati, J. M. Garcia Fernandez, *Org. Biomol. Chem.* **2015**, *13*, 1708–1723; g) K. Samanta, D. S. Ranade, A. Upadhyay, P. P. Kulkarni, C. P. Rao, *ACS Appl. Mater. Interfaces* **2017**, *9*, 5109–5117; h) N. Bono, C. Pennetta, A. Sganappa, E. Giupponi, F. Sansone, A. Volonterio, G. Candiani, *Int. J. Pharm.* **2018**, *549*, 436–445; i) R. V. Rodik, A.-S. Anthony, V. I. Kalchenko, Y. Mély, A. S. Klymchenko, *New J. Chem.* **2015**, *39*, 1654–1664;

- j) R. V. Rodik, A. S. Klymchenko, Y. Mely, V. I. Kalchenko, *J. Inclusion Phenom. Macrocyclic Chem.* **2014**, *80*, 189–200.
- [128] a) F. Sansone, M. Dudic, G. Donofrio, C. Rivetti, L. Baldini, A. Casnati, S. Cellai, R. Ungaro, *J. Am. Chem. Soc.* **2006**, *128*, 14528–14536; b) V. Bagnacani, F. Sansone, G. Donofrio, L. Baldini, A. Casnati, R. Ungaro, *Org. Lett.* **2008**, *10*, 3953–3956; c) V. Bagnacani, V. Franceschi, L. Fantuzzi, A. Casnati, G. Donofrio, F. Sansone, R. Ungaro, *Bioconjugate Chem.* **2012**, *23*, 993–1002; d) M. Dudic, A. Colombo, F. Sansone, A. Casnati, G. Donofrio, R. Ungaro, *Tetrahedron* **2004**, *60*, 11613–11618.
- [129] V. Bagnacani, V. Franceschi, M. Bassi, M. Lomazzi, G. Donofrio, F. Sansone, A. Casnati, R. Ungaro, *Nat. Commun.* **2013**, *4*, 1721.
- [130] A. L. Barrán-Berdón, B. Yélamos, L. García-Rio, O. Domech, E. Aicart, E. Junquera, *ACS Appl. Mater. Interfaces* **2015**, *7*, 14404–14414.
- [131] R. V. Rodik, A. S. Klymchenko, N. Jain, S. I. Miroshnichenko, L. Richert, V. I. Kalchenko, Y. Mely, *Chem. Eur. J.* **2011**, *17*, 5526–5538.
- [132] S. Mochizuki, K. Nishina, S. Fujii, K. Sakurai, *Biomater. Sci.* **2015**, *3*, 317–322.
- [133] A. Bom, M. Bradley, K. Cameron, J. K. Clark, J. van Egmond, H. Feilden, E. J. MacLean, A. W. Muir, R. Palin, D. C. Rees, M.-Q. Zhang, *Angew. Chem. Int. Ed.* **2002**, *41*, 265–270; *Angew. Chem.* **2002**, *114*, 275–280.
- [134] a) G. Yu, X. Zhou, Z. Zhang, C. Han, Z. Mao, C. Gao, F. Huang, *J. Am. Chem. Soc.* **2012**, *134*, 19489–19497; b) M. Ma, Z. Xie, L. Kong, Z. Li, J. Liu, R. Chen, *J. Jinsen Med. Sci.* **2018**, *41*, 317–321.
- [135] a) R. Cacciapaglia, A. Casnati, L. Mandolini, A. Peracchi, D. N. Reinhardt, R. Salvio, A. Sartori, R. Ungaro, *J. Am. Chem. Soc.* **2007**, *129*, 12512–12520; b) L. Wang, L.-l. Li, Y.-s. Fan, H. Wang, *Adv. Mater.* **2013**, *25*, 3888–3898; c) S. Viola, G. M. L. Consoli, S. Merlo, F. Drago, M. A. Sortino, C. Geraci, *J. Neurochem.* **2008**, *107*, 1047–1055; d) V. S. Pires, F. Gaboriau, J. Guillon, S. Da Nascimento, A. Dassonville, G. Lescoat, V. Desplat, J. Rochette, C. Jarry, P. Sonnet, *J. Enzyme Inhib. Med. Chem.* **2006**, *21*, 261–270; e) F. M. Menger, J. W. Bian, E. Sizova, D. E. Martinson, V. A. Seredyuk, *Org. Lett.* **2004**, *6*, 261–264; f) T. Läppchen, R. P. M. Dings, R. Rossin, J. F. Simon, T. J. Visser, M. Bakker, P. Walhe, T. van Mourik, K. Donato, J. R. van Beijnum, A. W. Griffioen, J. Lub, M. S. Robillard, K. H. Mayo, H. Grüll, *Eur. J. Med. Chem.* **2015**, *89*, 279–295; g) D. Santos, J. Medeiros-Silva, S. Cegonho, E. Alves, F. Ramilo-Gomes, A. O. Santos, S. Silvestre, C. Cruz, *Tetrahedron* **2015**, *71*, 7593–7599; h) R. P. M. uzhidDings, J. I. Levine, S. G. Brown, L. Astorgues-Xerri, J. R. MacDonald, T. R. Hoye, E. Raymond, K. H. Mayo, *Invest. New Drugs* **2013**, *31*, 1142–1150; i) F. N. Pur, K. A. Dilmaghani, *Pharm. Chem. J.* **2016**, *50*, 80–82; j) E. De Silva, D. Ficheux, A. W. Coleman, *J. Inclusion Phenom. Macrocyclic Chem.* **2005**, *52*, 201–206; k) X. Chen, R. P. Dings, I. Nesmelova, S. Debbert, J. R. Haseman, J. Maxwell, T. R. Hoye, K. H. Mayo, *J. Med. Chem.* **2006**, *49*, 7754–7765.
- [136] a) R. Lamartine, M. Tsukada, D. Wilson, A. Shirata, *C. R. Chimie* **2002**, *5*, 163–169; b) M. Mourer, H. M. Dibama, P. Constant, M. Daffe, J.-B. Regnouf-de-Vains, *Bioorg. Med. Chem.* **2012**, *20*, 2035–2041.
- [137] M. Coimbra de Oliveira, F. Souza Reis, Â. de Fátima, T. Furtado Ferreira Magalhães, D. Letícia da Silva, R. Rodrigues Porto, G. Almeida Watanabe, C. Viviane Buzanello Martins, D. Leite da Silva, A. Lúcia Tasca Góis Ruiz, S. Antonio Fernandes, J. Ernesto de Carvalho, M. Aparecida de Resende Stoianoff, *Lett. Drug Des. Discovery* **2012**, *9*, 30–36.
- [138] G. M. L. Consoli, G. Granata, R. Picciotto, A. R. Blanco, C. Geraci, A. Marino, A. Nostro, *MedChemComm* **2018**, *9*, 160–164.
- [139] Y. Ali, N. M. Bunnori, D. Susanti, A. M. Alhassan, S. Abd Hamid, *Front. Chem.* **2018**, *6*, 210.
- [140] V. S. Sharma, H. K. Singh, R. H. Vekariya, A. S. Sharma, R. B. Patel, *ChemistrySelect* **2017**, *2*, 8596–8606.
- [141] S. C. Özkan, A. Yilmaz, E. Arslan, L. Acik, U. Sayin, E. G. Mutlu, *Supramol. Chem.* **2015**, *27*, 255–267.
- [142] G. U. Akkus, E. Al, S. E. Korcan, *Supramol. Chem.* **2015**, *27*, 522–526.
- [143] M. N. Soares, Jr., T. M. Gascon, F. L. A. Fonseca, K. S. Ferreira, I. A. Bagatin, *Mater. Sci. Eng. C* **2014**, *40*, 260–266.
- [144] A. M. Boukerb, A. Rousset, N. Galanos, J.-B. Mear, M. Thepaut, T. Grandjean, E. Gillon, S. Cecioni, C. Abderrahmen, K. Faure, D. Redelberger, E. Kipnis, R. Dessein, S. Havet, B. Darblade, S. E. Matthews, S. de Bentzmann, B. Guery, B. Cournoyer, A. Imberty, S. Vidal, *J. Med. Chem.* **2014**, *57*, 10275–10289.
- [145] M. Dilek, K. Kadıyıcı, T. Tomek, E. Korcan, *J. Macromol. Sci. Part A* **2013**, *50*, 844–854.
- [146] M. B. Patel, N. R. Modi, J. P. Raval, S. K. Menon, *Org. Biomol. Chem.* **2012**, *10*, 1785–1794.
- [147] a) M. Mourer, R. E. Duval, C. Finance, J. B. Regnouf-De-Vains, *Bioorg. Med. Chem. Lett.* **2006**, *16*, 2960–2963; b) M. Grare, M. Mourer, S. Fontanay, J.-B. Regnouf-de-Vains, C. Finance, R. E. Duval, *J. Antimicrob. Chemother.* **2007**, *60*, 575–581; c) M. Mourer, H. M. Dibama, S. Fontanay, M. Grare, R. E. Duval, C. Finance, J.-B. Regnouf-de-Vains, *Bioorg. Med. Chem.* **2009**, *17*, 5496–5509; d) G. Sautrey, M. Orlof, B. Korchowiec, J.-B. R. de Vains, E. Rogalska, *J. Phys. Chem. B* **2011**, *115*, 15002–15012.
- [148] G. M. L. Consoli, G. Granata, V. Cafiso, S. Stefani, C. Geraci, *Tetrahedron Lett.* **2011**, *52*, 5831–5834.
- [149] G. M. L. Consoli, G. Granata, E. Galante, I. Di Silvestro, L. Salafia, C. Geraci, *Tetrahedron* **2007**, *63*, 10758–10763.
- [150] M. Mourer, N. Psychogios, G. Laumond, A.-M. Aubertin, J.-B. Regnouf-de-Vains, *Bioorg. Med. Chem.* **2010**, *18*, 36–45.
- [151] L. K. Tsou, G. E. Dutschman, E. A. Gullen, M. Telpoukhovskaya, Y.-C. Cheng, A. D. Hamilton, *Bioorg. Med. Chem. Lett.* **2010**, *20*, 2137–2139.
- [152] a) Z.-G. Luo, Y. Zhao, C. Ma, X.-M. Xu, X.-M. Zhang, N.-Y. Huang, H.-Q. He, *Chin. Chem. Lett.* **2014**, *25*, 737–740; b) Z. Luo, Y. Zhao, C. Ma, Z. Li, X. Xu, L. Hu, N. Huang, H. He, *Arch. Pharm. Chem. Life Sci.* **2015**, *348*, 206–213.
- [153] a) S. André, C. Grandjean, F.-M. Gautier, S. Bernardi, F. Sansone, H.-J. Gabius, R. Ungaro, *Chem. Commun.* **2011**, *47*, 6126–6128; b) S. Cecioni, S. E. Matthews, H. Blanchard, J.-P. Praly, A. Imberty, S. Vidal, *Carbohydr. Res.* **2012**, *356*, 132–141.
- [154] I. Morbioli, V. Porkolab, A. Magini, A. Casnati, F. Fieschi, F. Sansone, *Carbohydr. Res.* **2017**, *453*, 454, 36–43.
- [155] a) A. Yousaf, S. Abd Hamid, N. M. Bunnori, A. A. Ishola, *Drug Des. Dev. Ther.* **2015**, *9*, 2831–2838; b) C. Geraci, G. M. L. Consoli, G. Granata, E. Galante, A. Palmigiano, M. Pappalardo, S. D. Di Puma, A. Spadaro, *Bioconjugate Chem.* **2013**, *24*, 1710–1720; c) C. Geraci, G. M. L. Consoli, E. Galante, E. Bousquet, M. Pappalardo, A. Spadaro, *Bioconjugate Chem.* **2008**, *19*, 751–758; d) L. Latxague, F. Gaboriau, O. Chassande, J.-M. Léger, V. Pires, P. Rouge, A. Dassonville-Klimpt, S. Fardeau, C. Jarry, G. Lescoat, J. Guillon, P. Sonnet, *J. Enzyme Inhib. Med. Chem.* **2011**, *26*, 204–215; e) J. Z. Sun, M. A. Blaskovich, R. K. Jain, F. Delarue, D. Paris, S. Brem, M. Wotoczek-Obadia, Q. Lin, D. Coppola, K. H. Choi, M. Mullan, A. D. Hamilton, S. M. Sebiti, *Cancer Res.* **2004**, *64*, 3586–3592; f) J. Z. Sun, D. A. Wang, R. K. Jain, A. Carie, S. Paquette, E. Ennis, M. A. Blaskovich, L. Baldini, D. Coppola, A. D. Hamilton, S. M. Sebiti, *Oncogene* **2005**, *24*, 4701–4709.
- [156] L. An, L.-L. Han, Y.-G. Zheng, X.-N. Peng, Y.-S. Xue, X.-K. Gu, J. Sun, C.-G. Yan, *Eur. J. Med. Chem.* **2016**, *123*, 21–30.

- [157] A. Rescifina, C. Zagni, P. G. Mineo, S. V. Giofre, U. Chiacchio, S. Tommasone, C. Talotta, C. Gaeta, P. Neri, *Eur. J. Org. Chem.* **2014**, 7605–7613.
- [158] H. Zhou, D. A. Wang, L. Baldini, E. Ennis, R. Jain, A. Carie, S. M. Sebti, A. D. Hamilton, *Org. Biomol. Chem.* **2006**, 4, 2376–2386.
- [159] R. P. M. Dings, X. Chen, D. M. E. I. Hellebrekers, L. I. van Eijk, Y. Zhang, T. R. Hoye, A. W. Griffioen, K. H. Mayo, *J. Natl. Cancer Inst.* **2006**, 98, 932–936.
- [160] a) R. P. M. Dings, M. C. Miller, I. Nesmelova, L. Astorgues-Xerri, N. Kumar, M. Serova, X. Chen, E. Raymond, T. R. Hoye, K. H. Mayo, *J. Med. Chem.* **2012**, 55, 5121–5129; b) L. Astorgues-Xerri, M. E. Riveiro, A. Tijeras-Raballand, M. Serova, G. A. Rabinovich, I. Bieche, M. Vidaud, A. de Gramont, M. Martinet, E. Cvitkovic, S. Faire, E. Raymond, *Eur. J. Cancer* **2014**, 50, 2463–2477; c) N. A. Koonce, R. J. Griffin, R. P. M. Dings, *Int. J. Mol. Sci.* **2017**, 18, 2671–2679.
- [161] M. Zucchetti, K. Bonezzi, R. Frapolli, F. Sala, P. Borsotti, M. Zangarini, E. Cvitkovic, K. Noel, P. Ubezio, R. Giavazzi, M. D'Incalci, G. Taraboletti, *Cancer Chemother. Pharmacol.* **2013**, 72, 879–887.
- [162] R. Kamada, W. Yoshino, T. Nomura, Y. Chuman, T. Imagawa, T. Suzuki, K. Sakaguchi, *Bioorg. Med. Chem. Lett.* **2010**, 20, 4412–4415.
- [163] K. J. Pelizzaro-Rocha, M. B. de Jesus, R. R. Ruela-de-Sousa, C. V. Nakamura, F. S. Reis, A. de Fatima, C. V. Ferreira-Halder, *Biochim. Biophys. Acta Mol. Cell Res.* **2013**, 1833, 2856–2865.
- [164] K. Wang, D.-S. Guo, H.-Q. Zhang, D. Li, X.-L. Zheng, Y. Liu, *J. Med. Chem.* **2009**, 52, 6402–6412.
- [165] G.-F. Wang, X.-L. Ren, M. Zhao, X.-L. Qiu, A.-D. Qi, *J. Agric. Food Chem.* **2011**, 59, 4294–4299.
- [166] X. Zhang, Q. Cheng, L. Li, L. Shangguan, C. Li, S. Li, F. Huang, J. Zhang, R. Wang, *Theranostics* **2019**, 9, 3107–3121.
- [167] a) E. Ozylilmaz, S. Sayin, *Polycyclic Aromat. Compd.* **2018**, 38, 272–281; b) O. Sahin, S. Erdemir, A. Uyanik, M. Yilmaz, *Appl. Catal. A* **2009**, 369, 36–41; c) S. Erdemir, M. Yilmaz, *J. Mol. Catal. B: Enzym.* **2009**, 58, 29–35.
- [168] S. Cherenok, A. Vovk, I. Muravyova, A. Shivanyuk, V. Kukhar, J. Lipkowski, V. Kalchenko, *Org. Lett.* **2006**, 8, 549–552.
- [169] a) S. Sayin, E. Yilmaz, M. Yilmaz, *Org. Biomol. Chem.* **2011**, 9, 4021–4024; b) A. Uyanik, N. Sen, M. Yilmaz, *Bioresour. Technol.* **2011**, 102, 4313–4318; c) A. Uyanik, N. Sen, M. Yilmaz, *Polycyclic Aromat. Compd.* **2016**, 36, 613–627; d) E. Ozylilmaz, S. Sayin, *Appl. Biochem. Biotechnol.* **2013**, 170, 1871–1884; e) E. Ozylilmaz, M. Bayrakci, M. Yilmaz, *Bioorg. Chem.* **2016**, 65, 1–8; f) H. Yildiz, E. Ozylilmaz, A. A. Bhatti, M. Yilmaz, *Bioprocess Biosyst. Eng.* **2017**, 40, 1189–1196; g) S. Dutt, C. Wilch, T. Schrader, *Chem. Commun.* **2011**, 47, 5376–5383; h) E. Akoz, S. Sayin, S. Kaplan, M. Yilmaz, *Bioprocess Biosyst. Eng.* **2015**, 38, 595–604; i) S. Sayin, E. Akoz, M. Yilmaz, *Org. Biomol. Chem.* **2014**, 12, 6634–6642; j) T. A. Veklich, A. A. Shkrabak, N. N. Slinchenko, I. I. Mazur, R. V. Rodik, V. I. Boyko, V. I. Kalchenko, S. A. Kosterin, *Biochemistry (Moscow)* **2014**, 79, 417–424; k) I. D'Acquarica, A. Cerreto, G. Delle Monache, F. Subrizi, A. Boffi, A. Tafi, S. Forli, B. Botta, *J. Org. Chem.* **2011**, 76, 4396–4407; l) T. Mecca, G. M. L. Consoli, C. Geraci, F. Cunsolo, *Bioorg. Med. Chem.* **2004**, 12, 5057–5062; m) S. Francese, A. Cozzolino, L. Caputo, C. Esposito, M. Martino, C. Gaeta, F. Troisi, P. Neri, *Tetrahedron Lett.* **2005**, 46, 1611–1615; n) S. Cherenok, A. Vovk, I. Muravyova, A. Marcinowicz, J. Poznanski, O. Muzychka, V. Kukhar, W. Zielenkiewicz, V. Kalchenko, *Phosphorus Sulfur Silicon Relat. Elem.* **2008**, 183, 638–639; o) V. V. Trush, S. O. Cherenok, V. Y. Tanchuk, V. P. Kukhar, V. I. Kalchenko, A. I. Vovk, *Bioorg. Med. Chem. Lett.* **2013**, 23, 5619–5623; p) M. C. Semedo, A. Karmali, P. D. Barata, J. V. Prata, *J. Mol. Catal. B* **2010**, 62, 96–103; q) A. Marra, R. Zelli, G. D'Orazio, B. La Ferla, A. Dondoni, *Tetrahedron* **2014**, 70, 9387–9393; r) I. A. Veesar, I. B. Solangi, S. Memon, *Bioorg. Chem.* **2015**, 60, 58–63; s) J. Lee, L. Perez, Y. Liu, H. Wang, R. J. Hooley, W. Zhong, *Anal. Chem.* **2018**, 90, 1881–1888; t) M. G. Chini, S. Terracciano, R. Riccio, G. Bifulco, R. Ciao, C. Gaeta, F. Troisi, P. Neri, *Org. Lett.* **2010**, 12, 5382–5385; u) S. E. Sestito, F. A. Facchini, I. Morbioli, J.-M. Billod, S. Martin-Santamaria, A. Casnati, F. Sansone, F. Peri, *J. Med. Chem.* **2017**, 60, 4882–4892; v) E. V. Lugovskoy, P. G. Gritsenko, T. A. Koshel, I. O. Koliesnik, S. O. Cherenok, O. I. Kalchenko, V. I. Kalchenko, S. V. Komisarenko, *FEBS J.* **2011**, 278, 1244–1251; w) S. Gordo, V. Martos, E. Santos, M. Menendez, C. Bo, E. Giralt, J. de Mendoza, *Proc. Natl. Acad. Sci. USA* **2008**, 105, 16426–16431; x) S. Gordo, V. Martos, M. Vilaseca, M. Menendez, J. de Mendoza, E. Giralt, *Chem. Asian J.* **2011**, 6, 1463–1469; y) H. F. Allen, K. D. Daze, T. Shimbo, A. Lai, C. A. Musselman, J. K. Sims, P. A. Wade, F. Hof, T. G. Kutateladze, *Biochem. J.* **2014**, 459, 505–512.
- [170] Z. Wang, S. Tao, X. Dong, Y. Sun, *Chem. Asian J.* **2017**, 12, 341–346.
- [171] M. N. Shinde, N. Barooah, A. C. Bhasikuttan, J. Mohanty, *Chem. Commun.* **2016**, 52, 2992–2995.
- [172] J. Gao, D.-S. Guo, *Sci. Sin.* **2019**, 49, 811–820.

Manuscript received: December 20, 2019

Accepted manuscript online: January 21, 2020

Version of record online: October 13, 2020